EXPERIMENTAL ANALYSIS OF ROTATION IN A VERTICAL PLANE OF SHALLOW PIER FOUNDATIONS SUBJECTED TO A COUPLE

By

GEORGE BURNS WELCH

Bachelor of Science
Mississippi State University
State College, Mississippi
1947

Master of Science
Texas A and M University
1950

Submitted to the Faculty of the Graduate School of
the Oklahoma State University
in partial fulfillment of the requirements
for the degree of
DOCTOR OF PHILOSOPHY
August, 1965

EXPERIMENTAL ANALYSIS OF ROTATION IN A
VERTICAL PLANE OF SHALLOW PIER
FOUNDATIONS SUBJECTED
TO A COUPLE

Thesis Approved:

Thesis Adviser

Dean of the Graduate School

PREFACE

This investigation was conducted as a part of the Oklahoma Agricultural Experiment Station Project 633.

I am grateful for the privilege of working under Dr. G. L. Nelson, who served as Major Advisor. I express my most sincere appreciation to Dr. Nelson for advice, consultation, and inspiration through all phases of the work.

I wish to thank Professor E. W. Schroeder, Head of the Agricultural Engineering Department, Professor Jay G. Porterfield of the Agricultural Engineering Department, and Dr. R. L. Janes of the Civil Engineering Department for serving on the Advisory Committee. Their assistance and suggestions were appreciated.

Appreciation is extended to Albert Mink, Don McCrackin, and Dr. L. O. Roth for their assistance. Personnel of the research laboratory contributed considerably in building special equipment.

I am particularly grateful to Beth, my wife, and Eric, my son, for the sacrifices they made during this study.

TABLE OF CONTENTS

LIST OF TABLES

LIST OF FIGURES

Figures | Page

CHAPTER I

INTRODUCTION

Background

Rigid structural frames are used in many kinds of light structures for agriculture and other industries. The unobstructed overhead space afforded by this type building makes it particularly suitable for the installation of processing equipment and for the storage of farm equipment and feed supplies such as hay. An economical foundation for this type of structure can be obtained by extending the lower end of the vertical members into a concrete socket or pier of suitable depth into the ground.

The behavior of shallow piers subjected to an overturning moment is similar to the behavior of embedded poles used in pole-type structures and for supporting signs and electrical power lines. Reference will frequently be made to investigations pertaining to the stability of embedded piles and poles.

The foundation for a pole or rigid frame structure will tend to rotate when it receives an overturning moment from the pole or rigid frame reactions. The rotation of the piers in a structure with a floor in contact with the piers is resisted by both the floor and surrounding soil. The rotation of the piers in a structure without a floor or other means of increasing the stability is resisted only by the load bearing characteristics of the surrounding soil. This investigation is concerned with pier foundations which are supported only by the surrounding soil.

It would be very helpful if the designer could determine the amount of rotation that would occur when such a foundation is subjected to an overturning moment. It would be desirable to have a theoretical analysis for determining the rotation, but this has not yet been achieved. The major difficulty is the lack of a satisfactory time-related soil modulus. Because some soils will continue to deform under constant load, the deformation increases and the soil modulus varies with time. The rotation of a pier requires that large deformations occur near the ground surface in the direction of movement where the soil offers little resistance. Therefore, the soil near the ground surface will nearly always be in a plastic state (on the verge of failure) when resisting the rotation of a pier. At some depth below the surface, the soil behavior becomes more elastic. Prakash (1960) stated that a combination of elastic and plastic soil behavior should be accounted for in an analysis of embedded poles subjected to lateral loads.

Numerous authors have presented equations for determining the deflection of piles and embedded poles subjected to lateral loads. The application of these equations to the foundations of farm structures is somewhat limited because the depths assumed in the analysis are usually greater than those ordinarily used for farm structures. The assumption of loading until shear failure occurs in the soil, and complete overturning of the foundation would not be applicable to farm structures because this amount of movement would result in serious structural damage to the buildings.

The method of dimensional analysis has been used successfully for many years in the study of fluid mechanics. Beckett (1958) and Kondner (1962) have shown that this method can also be used successfully in studying the rotation of model poles subjected to a horizontal load. The method of dimensional analysis enables one to develop a prediction equation for calculating the movement of pier foundations without making assumptions pertaining to the time-related soil modulus.

Objectives

The purpose of this work was to determine the movement of a shallow pier foundation embedded in a saturated clay and sand mixture and subjected to rotation produced by an overturning moment. The major objectives were:

1. To develop a prediction equation for determining the rotation of shallow pier foundations subjected to an overturning moment. The equation was developed by conducting experiments with

models and organized on the basis of similitude theory.

2. To validate the equation with data obtained in the laboratory with a prototype.
3. To determine the effect of repetitive loading on the rotation of shallow pier foundations.

Assumptions and Limitations

It was assumed that the results from an investigation conducted with models would be applicable to other geometrically similar foundations. The validity of this assumption depends upon the correct application of similitude and the selection of pertinent quantities.

It was necessary to impose the following limitations on the experiment in order to concentrate on specific factors:

1. The model piers were assumed to be rigid. Therefore, all the deflection would be in the deformation of the soil.
2. Saturated soil was used throughout the experiment. For a given compaction it was assumed the soil had minimum strength, and the maximum rotation of the pier was obtained from the applied moments. The design of a foundation for a rigid or pole-type structure would be governed by the condition that would result in maximum rotation. The

saturated condition also prevented any change of moisture content from occurring during a test.

3. The same compaction effort was used in preparing the soil samples.

CHAPTER II

LITERATURE REVIEW

Introduction

The stability of embedded poles has been of interest to engineers for many years. The first research work done on the stability of poles was sponsored by electric power companies and outdoor advertising agencies that were concerned about the stability of the poles for supporting power lines and signs. Some work was also done by state highway departments that were using short posts for guards along highways.

The problem of developing a prediction equation for lateral deflection of poles has been approached by analytical derivation, full-scale tests, and model studies. A review of some of the work by each of these methods is given.

Rational Developments

Since the early 1920's, a number of papers have been presented that attempt to solve the laterally loaded pole problem. According to Prakash (1960), most of these solutions were based upon one or more of the following assumptions:

1. The maximum resistance to deformation of the soil at any depth is equal to Rankine's passive pressure or the difference between Rankine's passive and active pressure at that depth.
2. In order to develop passive resistance, there must be a movement, however small, of the member compressing the ground in front of it.
3. The intensity of passive resistance developed is proportional to the amount of the forward movement.
4. The intensity of the passive resistance developed is proportional to the depth below the surface of the ground.

The active and passive earth pressures are defined as follows:

Active pressure is the minimum earth pressure which will result on a vertical surface which is moving away from the soil mass.

Passive pressure is the limiting pressure which results on a vertical surface which is moving into a soil mass.

The equations for determining these pressures are:

$$P_a = -2C \tan(45-\phi/2) + GZ \tan^2(45-\phi/2)$$

$$P_p = 2C \tan(45+\phi/2) + GZ \tan^2(45+\phi/2)$$

where:

P_a = Active earth pressure, lbf./ft.^{2}

P_p = Passive earth pressure, lbf./ft.^{2}

C = Coefficient of cohesion, lbf./ft.^{2}

G = Weight of soil, lbf./ft.^{3}

Z = Depth, ft.

ϕ = Angle of internal friction

In an analysis by Seiler (1932), the soil pressures developed by a rotating pole are considered as the ordinates of a parabola whose position is such that the pressure area on one side of the pole bears the same relation to that on the other side as R does to P, these being the butt reactions, Figure 1.

$$W = P\frac{x}{y} \quad \text{and} \quad R = P + W$$

The ratio of R to P is not far from 1.1, and the pressure areas very closely satisfy this relation when the neutral axis occurs at a point 0.324d from the butt of the pole.

Empirical equations for computing the value of "P" were derived from data obtained in experiments conducted with full-size poles embedded in different classes of soil.

$P = 250d^{2.75}$ for "good to best" soils

$P = 125d^{2.75}$ for "average" soils

$P = 60d^{2.75}$ for "poor" soils

where:

P = Reactive force required to overturn pole, lbf.

d = Depth of embedment, ft.

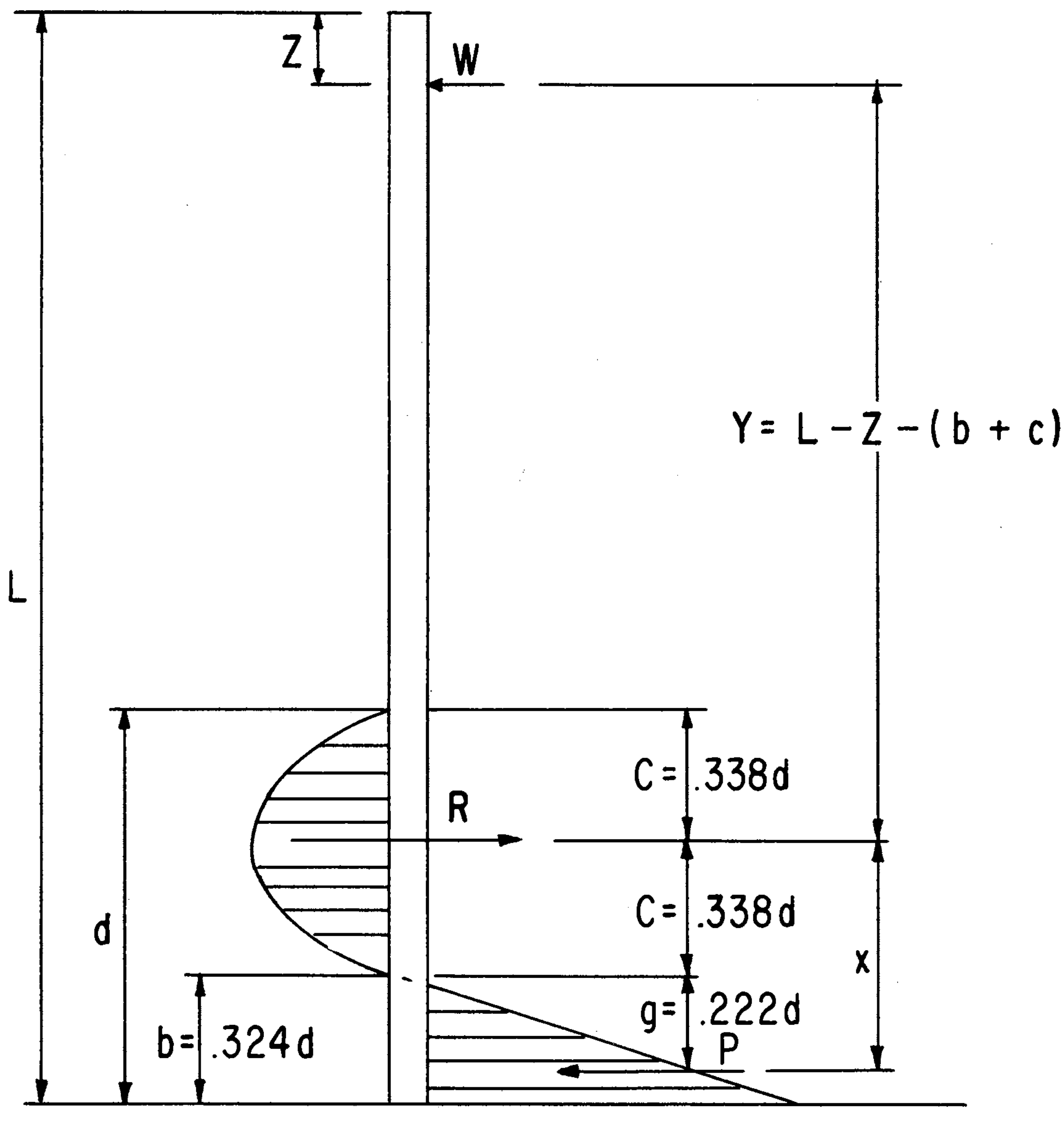

Figure 1. Example of Hypothetical Soil Pressure Pattern Acting on a Rotating Pole.

Substituting these values of "P" in the first equation above gives the following equations:

$$W = \frac{140d^{3.75}}{L-(Z+.662d)} \quad \text{for "good to best" soils}$$

$$W = \frac{70d^{3.75}}{L-(Z+.662d)} \quad \text{for "average" soils}$$

$$W = \frac{33.6d^{3.75}}{L-(Z+.662d)} \quad \text{for "poor" soils}$$

where:

W = Horizontal load acting on the pole, lbf.

L = Length of pole, ft.

Z = Distance from top of pole to horizontal load, ft.

Graphs were prepared to aid in determining the embedment depths for different lengths and classes of poles.

The soils were classified according to bearing capacity. The bearing capacity of the best soil was from 4 to 7 tons per square foot, or an average bearing capacity of 5 1/2 tons. That of the average soil from 2 to 4 tons, or an average of 3 tons, while poor soils ran from 1/2 to 2 tons, an average of 1 1/4 tons.

Appleford (1935) presented a solution to the pole embedment problem in the form of a nomograph for a pole one foot in width. It was assumed in his derivation that a horizontal movement of the pole will cause a wedge-shaped mass of soil to slide up a plane inclined 30 degrees in the direction of pressure and that the internal friction angle of the soil was 30 degrees. This method was being used by the Pacific Gas and Electric Company for determining pole embedment depths.

Griffith (1939) derived the following equation for determining the depth for setting poles:

$$L = 3.81 \sqrt{\frac{M_t}{dg}}$$

where:

L = Depth of pole setting, ft.

d = Diameter of pole foundation, ft.

M_t = Total moment at ground line, ft. lbf.

g = Maximum allowable soil resistance lbf./ft.^{2}

The procurement of site and soil data is of paramount importance, and the design pressures should be determined from these data. The allowable lateral soil resistance values for different classes of soil are usually determined by field tests and previous experience.

Abbett (1941) presented an analysis of the stability of cantilever poles in sandy soils. According to his analysis, a cone-shaped mass of soil is pushed out of the ground when the pole overturns. The resistance to rotation at the instant of impending motion comprises the forces of friction and cohesion acting on the surface of the cone. The resultant of these forces normal to the pole, therefore, must be proportional to the surface area of the cone.

Robbins (1957) developed a nomograph based on the assumption that the maximum soil resistance at any depth is the difference between the active and passive soil pressures at that depth. The graph was prepared from the following equation:

$$P_p - P_a = \frac{4W\ (2+3F)}{X^2}$$

where:

P_p = Total passive earth pressure, lbf./ft.^{2}

P_a = Total active earth pressure, lbf./ft.^{2}

W = Total horizontal load applied, lbf.

F = H/X

X = Depth of pole, ft.

H = Distance from load to ground surface, ft.

Nelidov (1957) developed a nomograph similar to the one presented by Robbins. It was based on the assumption that the soil reaction was parabolic in the upper two-thirds of the embedded length and triangular in the lower one-third.

Czerniak (1957) presented an extensive analysis of the resistance to the overturning of short piles. A short pile was defined as one whose embedded depth does not exceed ten times its least lateral dimension. For his analysis it was assumed that: (1) the pile is absolutely rigid; (2) the pile will rotate about a point somewhere along its length; and, (3) the soil resistance increases linearly with the depth.

The soil resistance was based on the following theory. When a short pile is rotated the horizontal pressure against the pile increases until it reaches the limiting value, known as the passive earth pressure. Further displacement of the pile does not significantly change the pressure. Before the passive pressure is reached, the body of the earth is in a state of elastic equilibrium and the magnitude of the pressure is related to the amount of pile movement. The movement, at the ground level, required to develop the passive earth pressure may be as high as 1/32 inch per foot of pile embedment. When the ultimate soil resistance is reached, the body of soil is in a state of plastic equilibrium and is on the verge of failure. The calculated value of this resistance, or passive pressure, when divided by a proper factor of safety, may be used in establishing the allowable lateral bearing pressure for design purposes. The general equation for determining the passive earth pressure was given earlier.

Equations were then derived from this theory for determining the actual soil pressures for round and rectangular piles.

1. Round Section

$$P_x = 9.425 \frac{H_o}{L} \left[-\left(\frac{4E}{L} + 3\right)\left(\frac{X}{L}\right) + 2\left(\frac{3E}{L} + 2\right)\left(\frac{X}{L}\right)^2 \right]$$

2. Rectangular Section

$$P_x = 6\,\frac{H_o}{L}\left[-\left(\frac{4E}{L} + 3\right)\left(\frac{X}{L}\right) + 2\left(\frac{3E}{L} + 2\right)\left(\frac{X}{L}\right)^2\right]$$

where:

P_x = Earth pressure against pile at distance X from ground surface, lbf./ft.^{2}

H_o = Lateral force per foot of pile diameter applied at the ground surface, lbf./ft. diameter

E = Distance from lateral load to ground surface, ft. (M_o/H_o)

L = Depth of pile measured from the ground surface, ft.

X = Distance between point at which P_x is taken and ground surface, ft.

M_o = Moment per foot of pile diameter applied at the ground surface, ft. lbf.

Nelson (1958) developed an equation for the deflection of an elastic pole subjected to tilting moments. It is necessary that the deflection due to anchorage yield be known. The assumptions used in the derivation were:

1. When the pole is loaded by a tilting moment, rotation occurs in a vertical plane about a fixed point between the butt of the pole and the ground line.

2. The horizontal reaction on the pole from earth or concrete in the pole anchorage during application of tilting moments has a distribution defined by a parabola with the axis horizontal.
3. Concrete used for backfilling the anchorage did not contribute to the stiffness of the pole.
4. Angular rotation of the pole in a vertical plane is small enough that changes in the geometry of loading caused by pole rotation are negligible.
5. The pole has the shape of a cylinder of uniform radius below grade and a tapered cylinder above grade such that the variation in 1/I is linear with distance from the bottom of the pole, where I is the moment of inertia of the pole cross section at any point.
6. The modulus of elasticity of the pole is constant.

The form of the equation is:

$$\phi = \frac{dy}{dx} = -\frac{\delta}{d} - \frac{\alpha^2 PD^2}{2EI}\left[\frac{\alpha^3}{15(2-3\alpha)} + \frac{1}{\gamma\alpha} + \frac{1}{3}\right]$$

where:

D = Total depth of pole, ft.

d = Distance between ground line and the point of rotation, ft.

H = Distance between ground line and point of applied load, ft.

δ = Ground line deflection, L

P = Lateral load, lbf.

Φ = Slope or angular rotation from vertical

$\alpha = \frac{d}{D}$ $\gamma = \frac{D}{H}$

The equation is applicable to the soil profiles comparable to the one in which the experiment was conducted.

The results of this analysis was validated by the data obtained in the experiment conducted by Nelson, Mahoney, and Fryrear (1956).

Prakash (1960) considered the additional effect of a vertical load and an initial inclination of the pole in an analysis of a rigid pole. The analysis was based upon a coefficient of horizontal subgrade reaction.

$$k_x = Kh \left(\frac{x}{L_s}\right)^n$$

where:

Kh = The value of k at the lower end of the pole

k = Coefficient of horizontal subgrade reaction for a pole of width B

$k = \frac{w}{y}$, FL^{-2}

k_x = Coefficient of horizontal subgrade reaction for pole at depth x, FL^{-2}

L_s = Embedded length of pole, L

n = An empirical exponent

$n = 1$ for sand

$n = .1$ for clay

w = Net soil reaction on beam of width B, FL^{-1}

x = Depth co-ordinate, L

y = Deflection co-ordinate, L

Equations were derived for soil reaction, critical buckling load, location of the axis of rotation, and moment and shear at any depth. According to Prakash, the calculated values of moment and of soil reaction agree with those obtained in tests conducted by Osterberg (1958).

Anderson (1948, 1960) made a study of the overturning of utility poles and cantilever supports for highway signs. The following equation was derived for the moment around the neutral axis per unit width of foundation.

$$M = 1/6\ aD^2 + 1/24\ bD^3$$

where:

$$a = 2C\left[\tan(45 + \phi/2) + \cot(45 + \phi/2)\right]$$

$$b = G\left[\tan^2(45 + \phi/2) - \cot^2(45 + \phi/2)\right]$$

C = Coefficient of soil cohesion, lbf./$ft.^2$

D = Depth of foundation, ft.

G = Weight of soil, lbf./$ft.^3$

ϕ = Angle of internal friction

The following assumptions were used in this derivation:

1. The resistance to motion is directly proportional to deflection.
2. The resistance to unit deflection varies with depth.
3. The above two relationships are straight line functions.

4. The net resistance of a soil to horizontal movement is the difference in the passive pressure and the active pressure.
5. The point of rotation is two-thirds of the depth below the surface.

In general, the most efficient foundation to resist a tilting moment is slim and deep, its slimness only limited by practical limitations such as internal strength and means of digging. The stability of a pole foundation can be increased by increasing the width of the top third of the embedded section at right angles to the direction of the force.

Walker and Cox (1964) developed an equation for the allowable lateral load acting on a pier.

$$H = \frac{6\ W\ a^2D^2 + 6\ W\ a\ b\ D^3 + W\ b^2D^4}{24\ aD + 18\ bD^2 + 36\ ha + 24\ hbD}$$

where:

H = Horizontal force, lbf.

h = Distance between surface and lateral force, ft.

W = Width of foundation, ft.

The other symbols are the same as those used by Anderson.

This equation was derived without making any assumption with regard to depth of rotation. It was shown in the derivation that the theoretical point of rotation occurs at a depth roughly corresponding to those observed experimentally, the mean value being approximately two-thirds of the depth from the surface.

The results of this equation and Anderson's (1960) equation showed that for 10-foot heights of loading the two equations yielded results within 3 per cent of each other in both sandy and clay soils. For heights of loading near the ground surface, Anderson's equation gave load values for clay soils within 1 per cent of the values obtained using Walker's equation but gave values approximately 10 per cent greater for sandy soils.

The validity of this equation was checked by comparing the calculated design loads with the results obtained from an experiment conducted on full-size piers 3/4,1, and 1 1/2 feet in diameter and set at depths of 2, 4, and 6 feet.

The comparison of the calculated and experimental design loads showed that, with the exception of the piers 2 feet deep which were loaded at a height of 10 feet, the equation predicted pier performance within 15 per cent accuracy. The theoretical design for the above pier was 25 per cent greater than the experimental value.

The experimental design loads were obtained by dividing the ultimate bearing capacity of the soil by a factor of three. In the test with the piers, it was assumed that the ultimate capacity was the load carried by the pier at 1/2 inch deflection 9 inches above the ground line.

The piers were undergoing considerable slippage at this deflection and, for all practical purposes, had failed. Terzaghi and Peck (1948), in their discussion of the foundation and footing settlement problems, indicate that the design load for a foundation system should not exceed one-third of the ultimate bearing capacity of the soil.

Effect of Cross-Sectional Shape

It would appear that the shape of a pole or pile would have some effect on its behavior. Different opinions have been reported in the literature.

Czerniak (1957) states that the maximum pressure against the middle element of a round pile is $\pi/2$ or 1.57 times the average on the projected area, or on a flat surface equal in width to the pile diameter. Since a curved surface can penetrate the earth easier than a flat surface, the effectiveness of a round pile must be decreased.

Shilts, Graves, and Driscoll (1948) reported that model poles 3 inches in diameter embedded in sand moved approximately 33 per cent more under a given load than a 3-inch square pole.

Williams (1952) conducted tests with round and square model piles 1, 2, 3, and 4 inches in size. It was found that the square-section piles could withstand only 90 per cent of the overturning moment withstood by circular-section piles. The form of the displaced soil wedge was similar for both cross-sectional shapes. The difference in resistance was credited to the effect of the curved periphery of the circular piles producing a consolidated arching of the sand, whereas the square-section pile tends to force its way through the sand.

Prakash (1961) reported that Davisson (1960) analyzed Nakamura's (1935) tests on model poles 6 centimeters wide in sand. The shapes studied were round, square, and diamond. The diamond shaped poles were actually square bars loaded along the diagonal, rather than along the side. According to this analysis, the shape of the cross section has negligible effect on the soil resistance and deflections.

Full-Scale Tests

The first experiments conducted on the stability of poles were made using full-size poles. This type of study involves considerable time and expense. Also, experiments conducted with full-size equipment can be cumbersome. The results are applicable only to the post-soil conditions similar to those in which the experiment was conducted.

Brownie and Fontaine (1929) conducted an experiment with approximately 100 poles of different species. The poles were about 30 feet long and embedded approximately 5 feet in the same manner as they would have been in power line construction. The soil at the test site was hard clay overlaid with 8 to 10 inches of sandy clay.

A horizontal load was applied until the poles failed. The poles broke off from 0 to 11 feet above the ground level. It was concluded from these tests that a depth of 4 1/2 feet for 30-foot poles was sufficient to develop the structural strength of the pole.

Krynine (1931) conducted a test in Russia in which wooden poles 3 to 3 1/2 inches in diameter, 6 to 7 1/2 feet long, were driven into a uniform clay with a moisture content of 17 to 18 per cent. A horizontal load was applied to each pole. The points of rotation were from 0.52D to 0.69D below the surface, where D is the depth of embedment. The poles driven beyond a depth of 20 to 22 inches failed structurally about 4 inches below the ground surface. The soil failed where the poles were embedded less than 22 inches.

Rutledge (1947) conducted extensive tests for the Outdoor Advertising Association. From this work a nomograph was developed for determining the required depth of embedment. A general classification of the soil can be made by a simple test at the construction site. The test is based on the force required to withdraw an auger from various depths. Five classifications are given for soils; namely, very soft, poor, average, good, and very hard. The values for the classes range in pounds per square foot from 800 to 1200; to 2000; to 3050; to 4100; and, to 4500 or above, respectively. Later tests made by Shilts and Graves (1948) validated the nomograph.

Nelson, Mahoney, and Fryrear (1956) conducted an experiment to determine the effects of horizontal loads on 6-inch poles projecting 14 feet above the ground. It was found that the depth of setting the poles is one of the important factors which control the stability of pole anchorages. Increasing the depth from 2 1/2 to 3 1/2 and 5 feet reduced movement to 38 per cent and 30 per cent, respectively, of the value at 2 1/2 feet. The effect of depth was most pronounced on deflection rates during the first application of the load. The recovery rate accompanying the removal of overturning moment was about 25 per cent greater for a 5-foot anchorage than for a 2 1/2-foot anchorage, and almost one-third greater for a 3 1/2-foot anchorage. Small increases in the water content of the soil around a pole anchorage can cause radical loss in stability in clayey soils. The effect of moisture is more pronounced for shallower anchorages.

It was suggested that pole rotation could be reduced by the following methods:

1. The use of concrete as compared to tamped earth for backfilling around the pole.
2. Increasing the depth of embedment.
3. Keeping the soil dry around the anchorage.
4. Preconsolidation of soil around the anchorages to increase the soil elastic modulus.

Hurst and Mason (1957) conducted a series of overturning and uplifting tests with steel and wood poles set at different depths and using soil, crushed stone, and concrete for backfill material. The results were analyzed statistically and indicated there was a significant difference in most of the treatments. They did not attempt to develop a prediction equation for determining deflection or uplift for other conditions.

Behn (1959) conducted tests with cylindrical footings 32 inches in diameter. The footings were set at 8 to 12-foot depths in a plastic, a granular, and an organic soil. Short-term tests were completed in three hours. Long-term tests lasted for 200 days or more. Results of the short-term tests indicate that the plastic and granular soils were similar in the strength characteristic as measured by resistance of the foundations to overturning. The long-term tests indicate that fixed loads about one-half as great as the maximum loads used in short-term tests produce about the same amount of tilt in a period of a year. Results of the tests were presented in tables and graphs of load versus deflection and rotation, and rotation versus time, respectively.

Model Studies

Since 1958 several studies using models and dimensional analysis have been made on the stability of poles and piles. Models have also been used in other investigations pertaining to soil mechanics. The use of models allows the experimental work to be conducted in the laboratory with a saving in time and expense. Also, better control of the experiment can be maintained with model studies.

Beckett (1958) conducted an investigation of the deflection of model poles embedded at different depths in loose sand, dense sand, and a saturated clay-sand mixture. The poles were subjected to increasing lateral loads until failure occurred. A prediction equation for computing the amount of deflection for each test was developed by dimensional analysis.

For loose sand:

$$Y = 1.824 \times 10^{-5} D(P/D^3\alpha)^{12.5} (D/H)^{0.68}$$

For dense sand:

$$Y = 1.68 \times 10^{-3} D \exp(5.5 P/D^{0.87} H^{2.13}\alpha)$$

For saturated clay-sand mixture:

$$Y/D = 632 (P/H^3\alpha)^{3.2546} (Kt/D)^{0.08009}$$

where:

Y = Horizontal deflection, L

D = Diameter of pole, L

P = Applied load, F

H = Depth of embedment, L

α = Weight of soil per unit volume, FL^{-3}

K = Permeability, LT^{-1}

t = Time, T

There was good agreement in the results obtained with model prototype poles and those computed by the prediction equation. These equations would be applicable to any size of pole provided they meet the requirements of dimensional analysis used in the test.

Rice (1959) conducted experiments with model poles to determine the effects of different anchorage designs on pole stability. The three types of anchorage used in the study are shown in Figure 2. The experiment was designed according to the principles of similitude. The tests were conducted in a tank filled with Ottawa sand.

The results indicate that the anchorage types with a wing were more resistant to rotation than the straight anchorage type. It was also found that a wing parallel to the direction of the applied force was more effective for a depth to diameter ratio of four than a wing normal to the direction of the applied force. A wing perpendicular to the direction of the applied force was more effective for a depth to diameter ratio of seven to nine.

Kondner and Green (1962) conducted tests with model poles embedded in dense sand and subjected to ground line thrust. The functional relationship was:

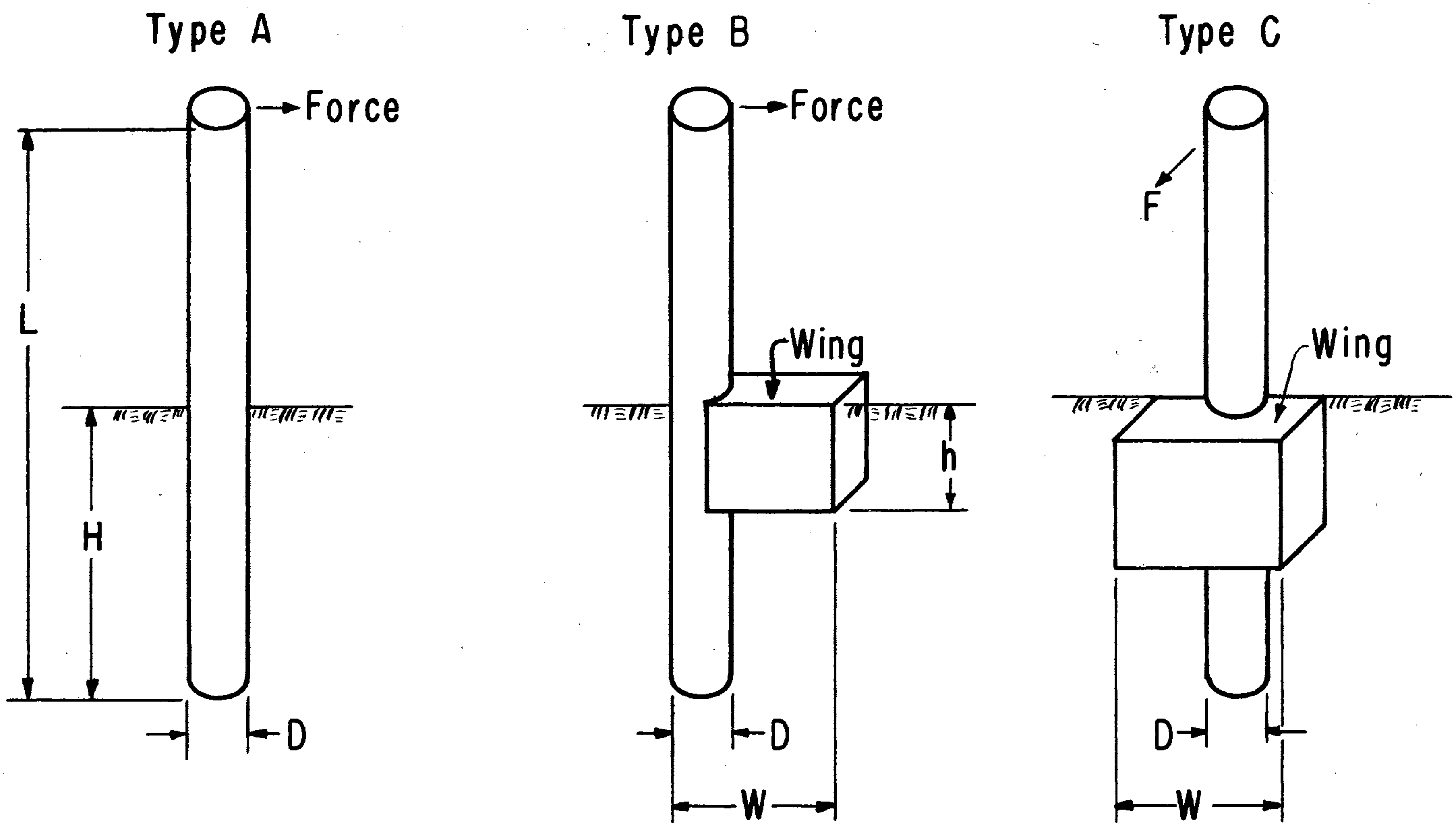

Figure 2. Anchorage Types for Fixed-End Arches.

$$Y/L = f(C/L,\ C^2/A,\ F/\alpha AL,\ \alpha tC/\eta,\ \phi)$$

where:

Y = Ground line thrust, L

L = Depth of embedment, L

A = Cross-sectional area of pole, L^2

C = Perimeter of pole, L

F = Thrust at ground line, F

α = Specific weight of sand, FL^{-3}

ϕ = Angle of internal friction

η = Viscosity of sand, $FL^{-2}T$

t = Time of loading, T

After applying certain restrictions and simplifying assumptions, the relationship reduced to:

$$Y/C = f(C/L,\ F/\alpha C^3)$$

the final prediction equation was:

$$Y/C = (.7-.5\ C/L)\ e^{3.28(C/L)^{2.24} F/\alpha C^3} - 1 \times 10^{-3}$$

Kondner, Krizek, and Schimming (1962) conducted a study with model poles embedded in sand and subjected to a couple. A prediction equation was derived for estimating the deflection.

Kondner and Cunningham (1963) conducted experiments with model poles embedded in sand and subjected to horizontal loads above the ground line. Hyperbolic prediction equations were derived from which the load-deflection characteristics of a prototype pole might be estimated.

CHAPTER III

EXPERIMENTAL DESIGN

Theory

An embedded pier-type foundation will rotate in a vertical plane when subjected to an overturning moment. The rotation of a pier in a saturated soil is resisted by the weight of the soil due to gravitational force, the depth of embedment, and the force necessary to deform the soil. The soil in front of the pier in the direction of movement above the point of rotation and at the back of the pier below the point of rotation is compressed when the pier rotates. This results in a decrease in the volume of the soil in these areas. Before a saturated soil can be deformed, some of the water must be squeezed from the voids in the soil to allow the soil particles to move closer together. The rate at which water will move through a soil is dependent upon the permeability. Therefore, it is hypothesized that the permeability is the controlling factor in this investigation.

It was assumed that the cohesive and shear strength of the soil would be negligible due to the high moisture content. Also, any movement due to the deformation of the individual soil particles would be very small compared to that caused by consolidation. For these reasons, these factors were omitted from the analysis.

Dimensional Analysis

It was mentioned earlier that some of the difficulties encountered when attempting to determine the rotation of a pier analytically can be circumvented by the method of dimensional analysis. This method was used in this experiment.

Dimensional analysis is an important tool in experimental work. Two advantages of dimensional analysis are: (1) saving of time and effort, and (2) greater generality in the equations defined by the experimental work. It is a method by which it is possible to describe all the important factors involved in a physical system by a single equation expressed in dimensionless parameters. Experiments are sometimes conducted in which all of the independent factors or variables considered in the investigation are varied through a selected set of values and their influence observed on a dependent variable. This procedure would result in several relationships when there are a number of independent variables. To understand the effect of the various factors affecting the physical system, the mathematical relationships among the variables would have to be defined. By the use of dimensional analysis, one mathematical relationship among the parameters may depict the entire relationship. The results obtained from various tests may appear to be different, but when examined in non-dimensional form may lead to the realization that some of the tests were in actuality duplications.

The method of dimensional analysis offers a means of simplifying experiments involving many variables and enables the researcher to obtain useful data with a minimum of experimental and computational effort. The method can be briefly summarized as follows: The quantities which are thought to have a measurable effect on the physical system are identified and analyzed dimensionally. The quantities are then combined into dimensionless ratios known as pi terms which can be treated as variables. The omission of a pertinent quantity may result in the analysis being ineffective; while the consideration of an unimportant factor may reduce the usefulness of the results and increase the required amount of experimentation. The number of pi terms required for a given set of quantities can usually be determined by the Buckingham Pi Theorem. This theorem states that the number of pi terms required to express a relationship among quantities in any physical system is equal to the number of quantities involved, minus the number of dimensions in which these quantities may be measured. However, there are some exceptions to this rule. Langhaar (1957) restated the theorem and showed that the number of pi terms required is always equal to the number of quantities involved minus the rank of the dimensional matrix for the quantities. There is no unique set of pi terms for a given set of quantities. Other pi terms can be formed by division or multiplication of the terms within the set. The only restriction placed on the pi terms is that they be dimensionless and independent.

An equation expressing the relationship of the pi terms can be written as

$$\pi_1 = f(\pi_2, \pi_3, \ldots \ldots \pi_n) \qquad 3\text{-}1$$

which involves an unknown function. To formulate a prediction equation, the nature of the function must be established. This cannot be done by dimensional analysis alone, but it may be done from analysis of laboratory observations. Murphy (1950) suggested the following procedure for determining the type of function and also for evaluating it. The observations are arranged so that all of the independent pi terms, except one, involved in the function remain constant. That one is varied to establish a relationship between it and the term being observed. The relationship established between the two terms is known as a component equation. The same procedure is repeated for each of the other independent pi terms. The relationships between the quantity being observed and each of the other pi terms can be combined to give a general relationship. If the observations plot as a straight line on log-log paper, the component equations are of the form $\pi_1 = A\,\pi_n^{a}$. The pi terms will combine by multiplication and the general prediction equation will have the form of the equation 3-2.

$$\pi_1 = K_1 \pi_2^{K2} \pi_3^{K3} \ldots \ldots \pi_n^{Kn} \qquad 3\text{-}2$$

If the observations plot as straight lines on arithmetic paper, the pi terms will combine by addition and will have the form of equation 3-3.

$$\pi_1 = K_1 f(\pi_2) + K_2 f(\pi_3) + \ldots + K_s f(\pi_s) + K \qquad 3\text{-}3$$

Triaxial Test

The first phase of this investigation was to design and conduct an experiment to study the strength of a clayey soil. This experiment was designed to use the consolidated-undrained triaxial test.

The quantities thought to be pertinent to the system are given in Table I.

TABLE I

PERTINENT QUANTITIES FOR TRIAXIAL TEST

No.	Symbol	Parameter	Dimensions
1	σ_1	Applied Stress, Kg./cm.^{2}	FL^{-2}
2	σ_3	Confining Pressure, Kg./cm.^{2}	FL^{-2}
3	C	Cohesive Strength, Kg./cm.^{2}	FL^{-2}
4	ε	Strain	--

Writing the pi terms gives:

$$\pi_1 = \varepsilon \qquad \pi_3 = C/\sigma_3$$

$$\pi_2 = \sigma_1/\sigma_3$$

The general relationship among the pi terms is:

$$\varepsilon = f(\sigma_1/\sigma_3,\ C/\sigma_3) \qquad 3\text{-}4$$

Model and Prototype Pier Experiment

The second phase of this investigation was to design and conduct an experiment from which a prediction equation could be derived for predicting the rotation of a pier subjected to an overturning moment produced by a couple. With certain combinations of horizontal and vertical forces acting on a rigid frame structure, the resulting horizontal shearing force at the ground line is zero thus leaving only the overturning moment to act on the foundation. Also, the shearing force is often small enough that it has little effect as compared to the overturning moment. For example, a 2,000-pound vertical force acting at the center of a 40-foot rigid frame structure could produce a 12,200 foot-pounds moment and a 2,145-pound horizontal shearing force. The horizontal shearing force would have little effect on a pier 6 feet deep as compared to the overturning moment. However, the addition of a large horizontal shearing force to a pier subjected to an overturning moment would increase the rotation and would also cause translation of the pier.

Pertinent Quantities for the Model and Prototype Pier Experiment

The physical quantities believed to be pertinent to the rotation of a pier in a saturated soil are listed in Table II.

TABLE II

PERTINENT QUANTITIES FOR MODEL AND PROTOTYPE EXPERIMENT

No.	Symbol	Parameter	Dimensions
1	D	Diameter of Pier, in.	L
2	H	Depth of embedment, in.	L
3	ρ	Mass density of soil, lbm./in.^{3}	ML^{-3}
4	t	Elapsed time, min.	T
5	M	Moment at ground line, in.lbf.	FL
6	Θ	Angle of rotation	--
7	G	Gravitational force, lbf./lbm.	FM^{-1}
8	K	Permeability, in.^{4}/lbf.min.	$F^{-1}L^4T^{-1}$
9	N	Number of loading cycles	--
10	W	Water content	--
11	Ne	Newton's Second Law Coefficient	$FM^{-1}L^{-1}T^2$
12	C	Cohesive strength, lbf./in.^{2}	FL^{-2}
13	ϕ	Friction angle of soil	--

Dimensions: F = Force M = Mass

L = Length T = Time

Number of pi terms = 13-4 = 9

$\pi_1 = \Theta$

$\pi_2 = H/D$

$\pi_3 = M/G\rho DH^3$

$\pi_4 = KG\rho t/H$

$\pi_5 = N$

$\pi_6 = W$

$\pi_7 = Gt^2/NeH$

$\pi_8 = \phi$

$\pi_9 = C/G\rho H$

The general relationship among the pi terms is:

$$\Theta = f(H/D,\ M/G\rho DH^3,\ KG\rho t/H,\ N,\ W,\ Gt^2/NeH,\ \phi,\ C/G\rho H) \quad 3\text{-}5$$

Discussion of Pertinent Quantities

It was felt that the physical quantities listed in Table II were adequate for studying the rotation of a pier in a saturated soil.

Previous experiments have shown that depth (H) of embedment is one of the important factors which control the stability of pole anchorages. The diameter (D) and depth determine the soil area that the pier acts against and thereby affect the pressure distribution.

Before a saturated soil can be deformed, some of the water must be removed from the pores of the soil. The amount of water removed from the pores is dependent upon the permeability (K) and the length of time (t) the force is applied. The inertial forces developed by the water being accelerated is related to the system by Newton's coefficient (Ne).

It was shown in the preliminary work with the triaxial tests that the deformation of a soil in a constrained condition can be accounted for by the cohesive strength, the applied stress, and the confining pressure.

The friction angle of the soil, number of loading cycles, and water content are discussed in the following section on dimensionless ratios.

Discussion of Dimensionless Ratios

The laws of similitude do not specify how the pertinent quantities should be combined to give the best set of pi terms. The only requirement is that they be dimensionless and independent. In order to facilitate experimental work, the pi terms that appear to be most meaningful to the physical system should be selected. A discussion of the pi terms selected for this study follows.

$\pi_1 = \theta$ is the accumulated angle of rotation of the pier measured from the vertical. This is the dependent pi term and was measured as a function of the respective independent pi terms.

$\pi_2 = H/D$ is the ratio of the embedment depth to the diameter of the pier. The ratio was varied by varying the depth. The diameter was constant throughout the experiment. It was decided to vary the depth because this would be more convenient than varying the diameter. The values assigned to π_2 were 4, 5, 6, 7, 8, and 9. These values gave embedment depths of 3, 3 3/4, 4 1/2, 5 1/4, 6, and 6 3/4 inches, respectively, for piers 3/4 inch in diameter.

$\pi_3 = M/G\rho DH^3$ is an index of the ratio of the overturning moment to the resisting force developed by the weight of the soil. This parameter can be thought of as a strength ratio. This ratio was varied by varying the applied moment while the other quantities in the ratio were held constant. The values assigned to this parameter were 0.482, 0.964, 1.446, 1.928, and 2.410.

$\pi_4 = KG\rho t/H$ is a parameter designed to determine how the angle of rotation is influenced by the length of time that the moment acts on the pier. It is known from experiments and theory that the deformation of a clayey soil is related to the length of time the load is applied. The values assigned to this parameter were 0.0099, 0.0199, 0.0298, 0.0398, and 0.0796. The value of t in each of these values was 0.25, 0.50, 0.75, 1, and 2 minutes respectively.

This parameter is an index of the ratio of the gravity force to the pore water pressure developed in squeezing water out of the pores of the soil.

$\pi_5 = N$ is the number of loading and unloading cycles applied to the piers. The values assigned to this parameter were 1, 3, 5, 7, and 9.

The resistance to deformation of a soil is increased by repetitions of stress. The increase in strength can be attributed to increase in density, change in moisture distribution, development of thixotropic strength, and change in structural arrangement of the grains.

π_6 = W is the moisture content of the soil. This parameter was held constant at saturated conditions for all the tests; therefore, it was not included in the experimental design.

$\pi_7 = Gt^2/NeH$ is a form of the Froude number which is an index of ratio of inertial forces to gravitational forces developed on an element of fluid or soil being accelerated. The movement of the water would be slow as it is squeezed through the pores of the soil by a rotating pier. Inertial forces would be small and can be neglected.

$\pi_8 = \phi$ is the internal friction angle of the soil. This parameter would be constant since the same soil at a constant moisture content was used in all the tests; therefore, it can be omitted from the experimental design.

$\pi_9 = C/G\rho H$ is an index of the ratio of the cohesive strength to gravity forces. It was assumed that the cohesive strength of the soil would be negligibly small in comparison to gravity due to the high moisture content.

Previous work by Beckett (1958) has shown that for saturated soil conditions good correlation of experimental and calculated values can be obtained when cohesive strength and the internal friction angle of the soil are not included in the experimental design.

Chung (1965) reported that during shearing deformations the cohesive and frictional resistances develop independently. In general, the cohesion attains a peak value at low strain but decreases rapidly with an increase in water content. The angle of internal friction also decreases with an increase of water content, since the effect of dilatancy is reduced. The friction angles are small at low strains because these angles depend principally upon particle interference and the usual dilatancy which accompany larger displacements.

Eliminating four pi terms, equation 3-4 is reduced to:

$$\pi_1 = f(\pi_2, \pi_3, \pi_4, \pi_5) \qquad 3\text{-}5$$

To define experimentally a prediction equation, the experimental schedule of Table III was used.

Photographic Study

The final part of the study was to develop a soil deformation visualization device. The purpose of this device was to provide a means of observing and photographing the soil movement and deformation pattern developed when a pier rotates.

TABLE III

SCHEDULE OF EXPERIMENTS

Test No.	π_1 θ	π_2 H/D	π_3 $M/G\rho DH^3$	Moment in. lbs.	π_4 $KG\rho t/H$	Time Min.	π_5 N
1		4		2.0351		8.57	
2		5		3.9746		10.71	
3	Measure	6		6.8685		12.85	
4		7	1.4460	10.9069	0.5980	15.00	5
5		8		16.2810		17.14	
6		9		23.1813		19.28	
7			0.4820	3.6349			
8			0.9640	7.2699			
9*	Measure	7	1.4460	10.9069	0.5980	15.00	5
10			1.9280	14.5418			
11			2.4100	18.1768			
12*					0.0099	0.25	
13*					0.0199	0.50	
14*	Measure	7	1.4460	10.9069	0.0298	0.75	5
15*					0.0398	1.00	
16*					0.0796	2.00	
17*							1
18*							3
19*	Measure	7	1.4460	10.9069	0.5980	15.00	5
20*							7
21*							9

*Same as Test No. 4

CHAPTER IV

EXPERIMENTAL EQUIPMENT

Triaxial Testing Equipment

The triaxial testing equipment shown in Figure 3 was used to study the strength of the soil.

The triaxial test cylinder was connected to the water reservoir and pressure tank by a heavy duty pressure hose and valve. The pressure tank was used to maintain the desired confining pressure. The water reservoir was necessary to prevent air from entering the test cylinder. The pressure in the pressure tank and test cylinder equalized when the valve was opened.

The microdial measured the vertical displacement of the specimen under load.

Soil

The soil for the experiment consisted of a mixture of equal parts by weight of Ottawa Flint Shot sand and Permian clay. This was also approximately equal parts by volume. The clay was obtained along a road bank during the summer months and had a very low moisture content. It was then sifted through a 14 x 18 mesh wire screen to remove the

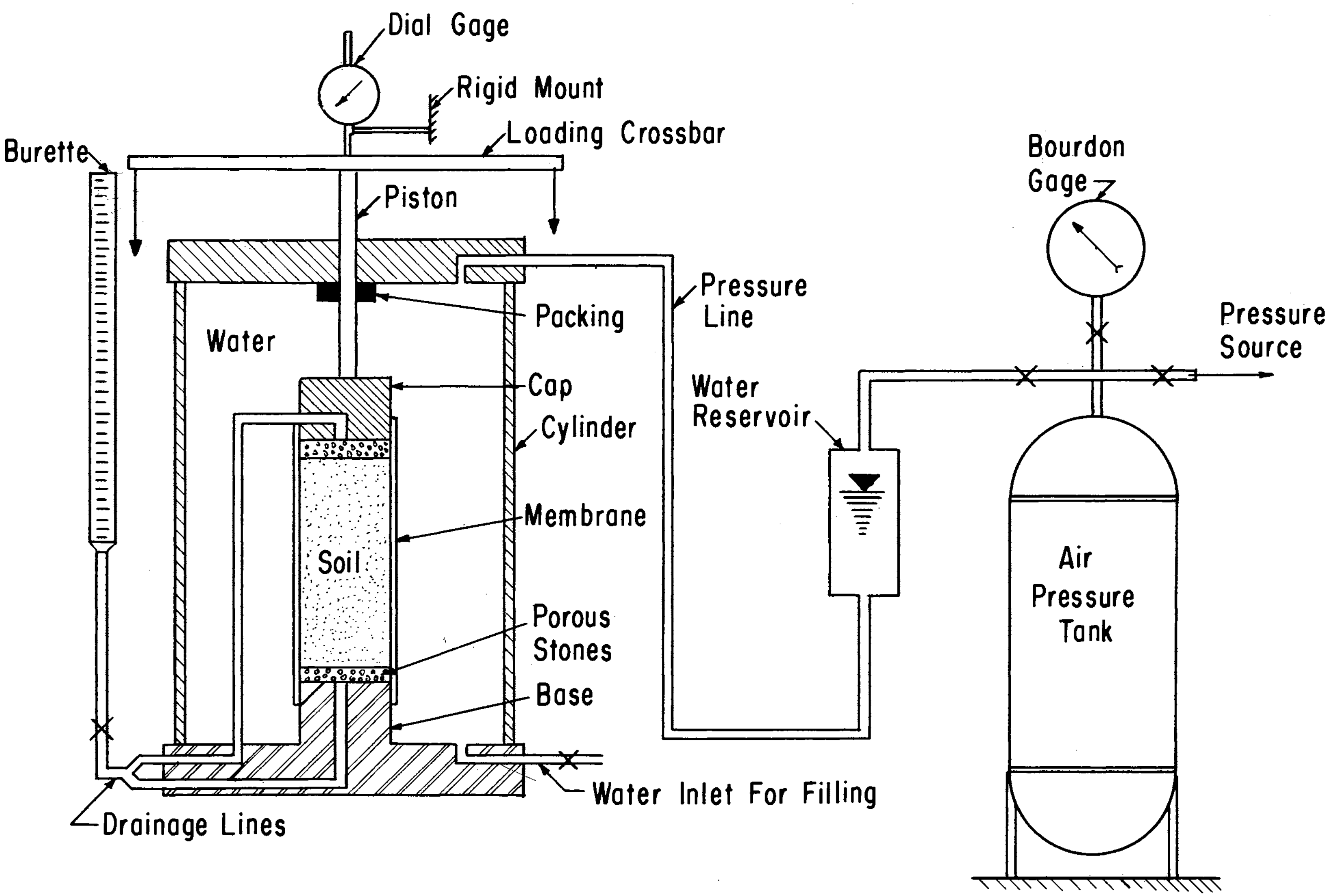

Figure 3. Triaxial Testing Equipment.

larger pieces of gravel and soil. The clay and sand were mixed in a large flat bottom metal tank. The dry soil was spread in thin layers and water sprinkled on it until enough water had been added to bring the moisture content up to approximately 9.5 per cent. The soil was then raked into a pile and covered with plastic for 12 hours. This was to allow the moisture to migrate through the soil enough so that further mixing could be achieved without the soil rolling into small mud balls. The soil was then placed in a barrel with a tight fitting cover to prevent any loss of moisture.

The permeability of the soil was determined with the apparatus shown in Figure 4. The soil was tamped in the permeameter in the same manner as for embedding a pier. The water was introduced to the sand at the bottom of the layer of soil. A constant head of 12 inches was maintained during the test. The top of the permeameter was covered with polyethylene plastic to minimize the evaporation of the water that flowed through the soil. The water flowing through the layer of soil was collected for 8 minutes and weighed. From this data, the permeability was calculated to be 3.012 inches^4 per pound force minute.

The density of the soil was determined by weighing the soil that had been tamped into a cylinder of known volume and then saturated. The density was 0.0695 pounds mass per inch^3. The moisture content was 26 per cent.

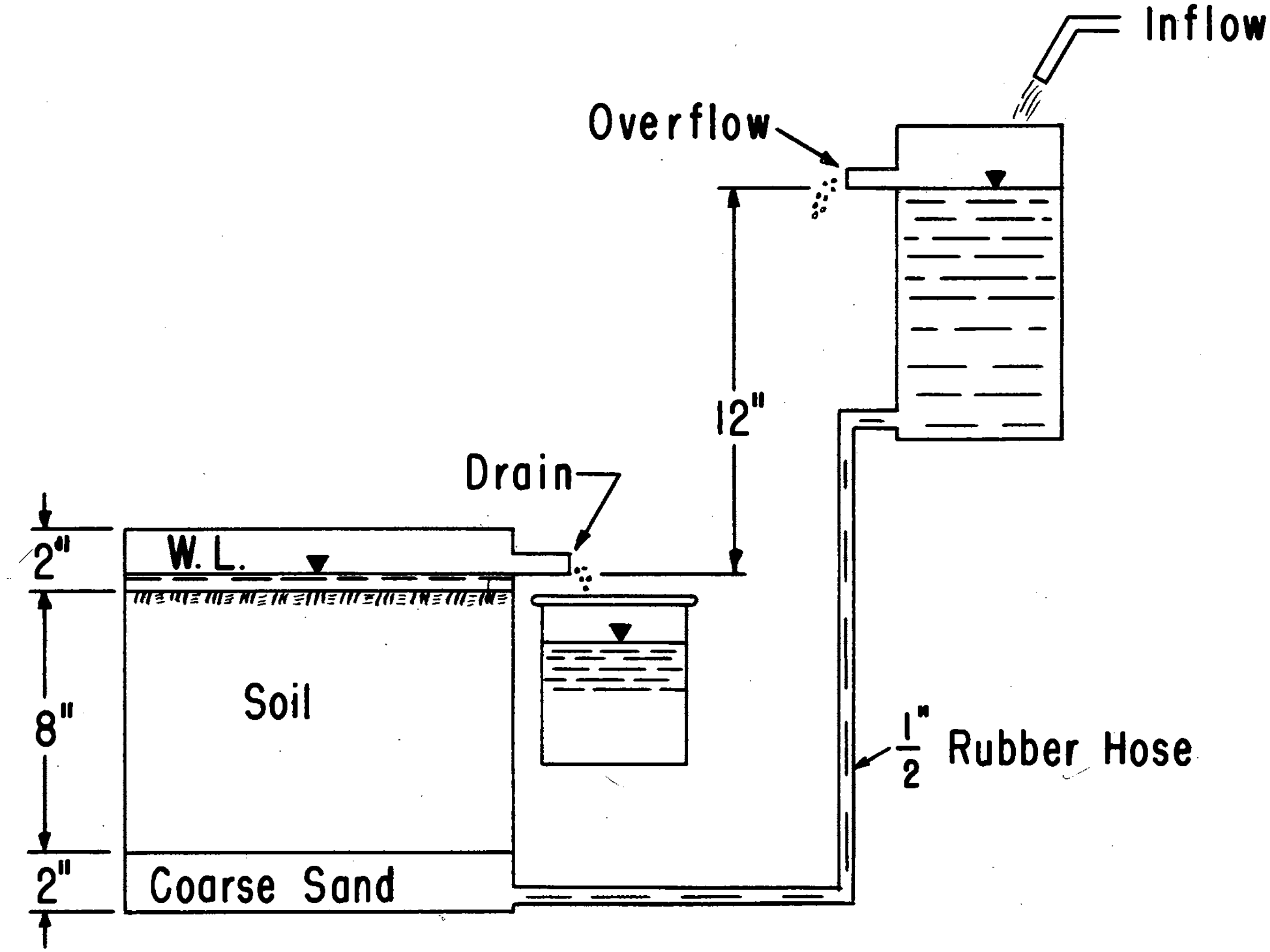

Figure 4. Apparatus Used to Determine the Permeability of the Soil.

Containers for Embedding Piers

Steel containers 14 inches in diameter and 15 inches deep were used for holding the soil in which the model piers were embedded. Using separate containers for the piers, prevented any interaction from occurring between the various tests. The walls of the containers were 1/8 inch thick and were rigid enough not to deflect when the piers rotated. The steel containers were embedded in sand in a box 6 x 3 x 1 1/2 feet. The box was constructed of 2-inch Redwood staves. Embedding the containers for the model piers in sand prevented any movement of the containers when the loads were applied to the piers. The weight of the box and sand also helped minimize any vibrations that might occur to the test equipment.

The container for the prototype was a section of a 55-gallon oil drum embedded in the same tank, Figure 6.

Model Piers

The model piers were made of low carbon steel. The lower portion was 3/4 inch in diameter. The upper portion was made of 1/8 x 3/4-inch flat bar.

The prototype pier was 1 1/2 inches in diameter with a 1/4 x 1 1/2-inch flat bar at the top.

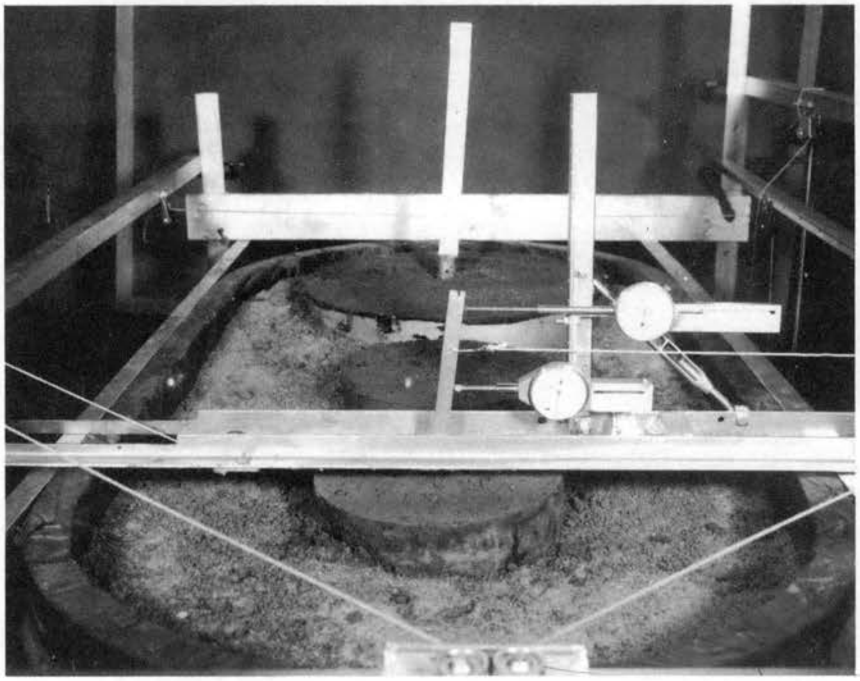

Figure 5. Model Pier Under Load.

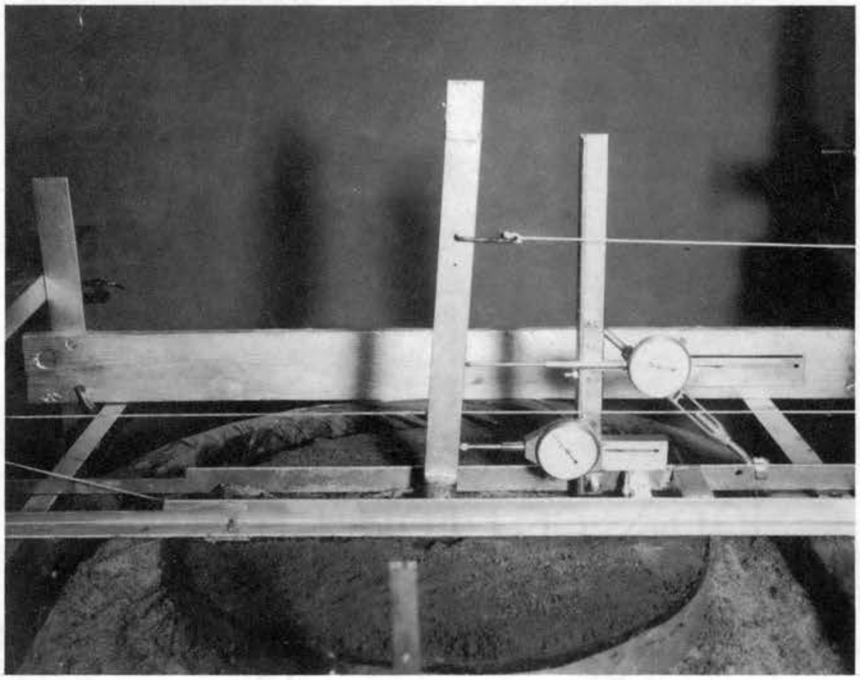

Figure 6. Prototype Pier Under Load.

Ames Dial Indicators

The rotation of the piers was measured with Ames Dial Indicators as shown in Figures 5 and 6. The dial scale was graduated in 0.001-inch divisions. The springs were removed from the dials to prevent the dials from exerting pressure against the piers.

The portable mount for the dials in shown in Figure 5. The dials were located 4 and 8 inches above the soil surface. A turnbuckle was used for bracing the vertical member supporting the dials. The turnbuckle was also used to adjust the position of the tips of the dials to fit closely against the arm of the pier.

Tamping Tool

The tamping tool used for compacting the soil is shown in Figure 7. The tool was provided with a stop and lock nut so that the spring displacement could be adjusted to give the desired compaction.

Soil Deformation Visualization Device

The device used in conducting the photographic study is shown in Figures 27 through 32. The container was a 12 x 12 x 10-inch box made of 1/4 inch clear plastic.

The pier was made from a piece of 1 x 1/2-inch steel channel. The edges of the channel were cut down to a

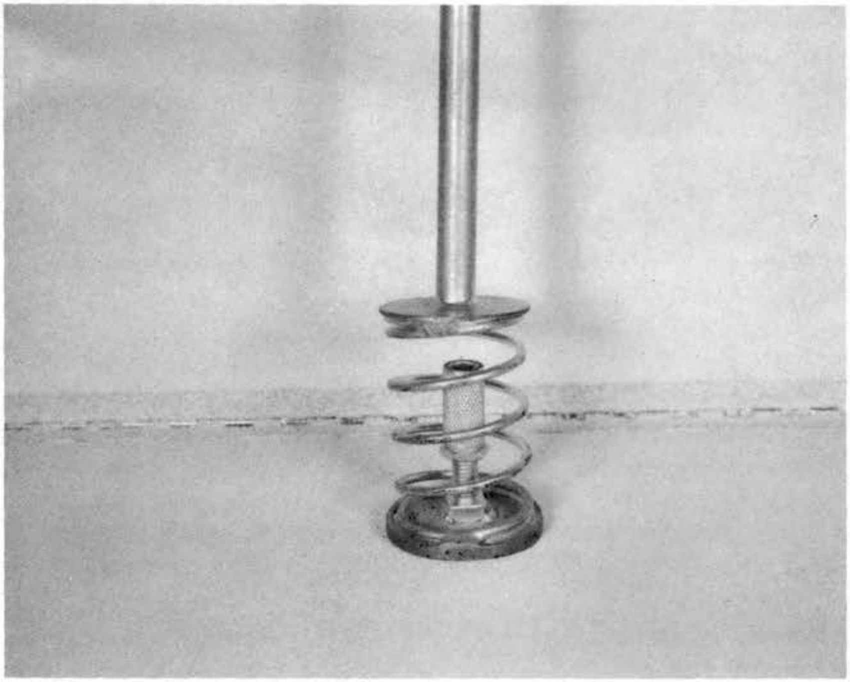

Figure 7. Tamping Tool Used for Packing the Soil.

thickness of 1/16 inch to provide better contact against the side of the box. A small plate was welded to the bottom of the channel to prevent sand from moving up into the pier.

The pier was pinned tightly against the side of the box. This was necessary to prevent the sand from flowing between the pier and the side of the box. The pivot point was located two-thirds of the embedment depth below the surface.

The grid was formed by placing a layer of white sand in the box, a 1/8-inch layer of black sand, and another layer of white sand. The vertical lines were formed by pushing an oilcan spout filled with black sand down to the layer of black sand. The spout was held at approximately 45 degrees. Moving the spout back and forth as it was brought upward along the side of the box, the black sand flowed out forming the vertical line. When all the vertical lines were completed for that layer, another layer of black sand and a layer of white sand were added. The vertical black lines were then added to this layer. The operation was continued in this sequence until the desired depth was obtained.

CHAPTER V

PROCEDURE

Triaxial Tests

The consolidated-undrained test was used in studying the strength of the soil. Tests were conducted on two mixtures of Permian clay and Ottawa sand. One mixture contained 40 per cent clay while the other one contained 50 per cent clay. The optimum moisture content of the two mixtures was 9.5 and 10 per cent, respectively, for the compaction given below.

The soil specimens were prepared at the optimum moisture content with a Harvard Miniature compaction mold. The spring loaded plunger was adjusted to give 20 pounds force on the tamper which was 1/2 inch in diameter.

The specimens were enclosed in rubber membranes and placed in the test cylinders. The confining pressure was applied and the specimens allowed to consolidate until the water ceased to rise in the burette tube which indicated that the specimens were fully consolidated. This usually required from 8 to 10 hours.

The valves on the test cylinder were closed at the beginning of the loading test. Load increments were applied at one-minute intervals. The deformation of the soil specimen was recorded from the dial gage 55 seconds after the application of the load.

The load was increased until the specimen failed.

The confining pressure used in the tests varied from .5 to 2 kilograms per square centimeter in increments of .5 kilogram. Three replications were made for each confining pressure.

Placement of Piers

All the tests were conducted in the laboratory with model and prototype piers and a prepared mixture of clay and sand.

The piers to be tested were rigidly suspended from a crossbar above the box, Figure 8. They projected into the steel containers by an amount equal to the embedment depth. The moist soil was placed in the containers in layers approximately one inch thick and tamped. The tamping tool was adjusted to give 4.5 pounds pressure per square inch. The same amount of compaction effort was used for each layer. The soil was tamped one time at a given spot on the surface. Soil was added until it was level with the top of the container. The suspension crossbar was then removed.

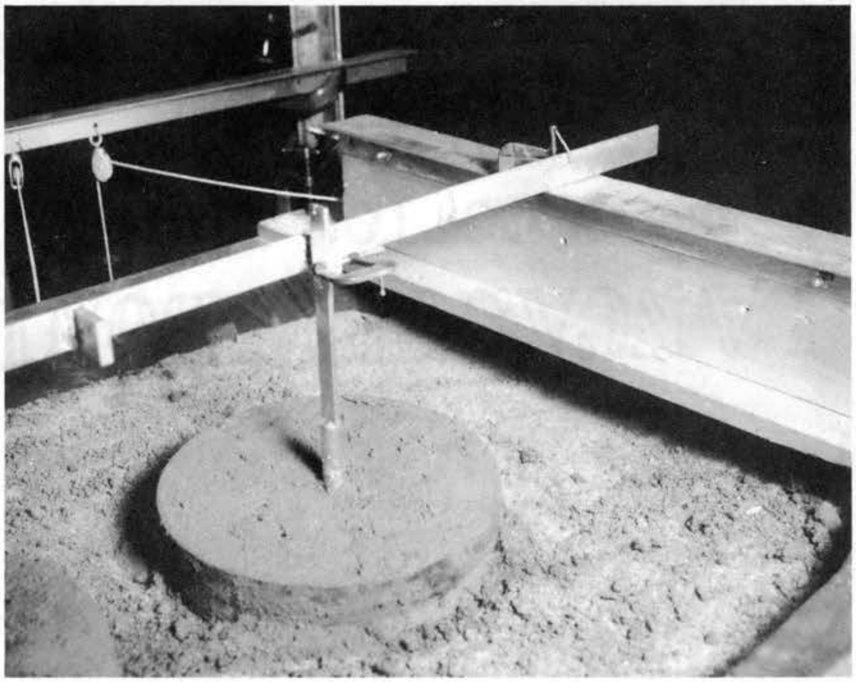

Figure 8. Method Used to Hold the Piers in Place while the Soil was Tamped.

Saturating the Soil

The soil was saturated by allowing water to flow onto the surface at a slow rate. The time required to saturate the soil was approximately 3 hours. The saturated soil was allowed to set for 24 hours before running the loading test.

Loading the Piers

The system for applying an overturning moment to the model piers is shown in Figure 9. Strings were attached to the pier at the soil surface and at a point 6 inches above the soil surface. The strings were then run horizontally over the pulleys A and B and then down to the cross beam. The cross-beam was weighed before running a test. The desired moment was obtained by placing additional weight increments on the beam. This system exerted equal forces in opposite direction on the pier to give the desired overturning moment.

The crossbeam was raised and lowered by two other strings attached to the beam and run through the pulleys C and D. The beam was in the raised position at the beginning of each loading cycle. The required weights were placed on the beam and then gently lowered.

The moment was applied to the piers for a predetermined period of time. The dial readings were recorded at regular intervals and from these the angle of rotation

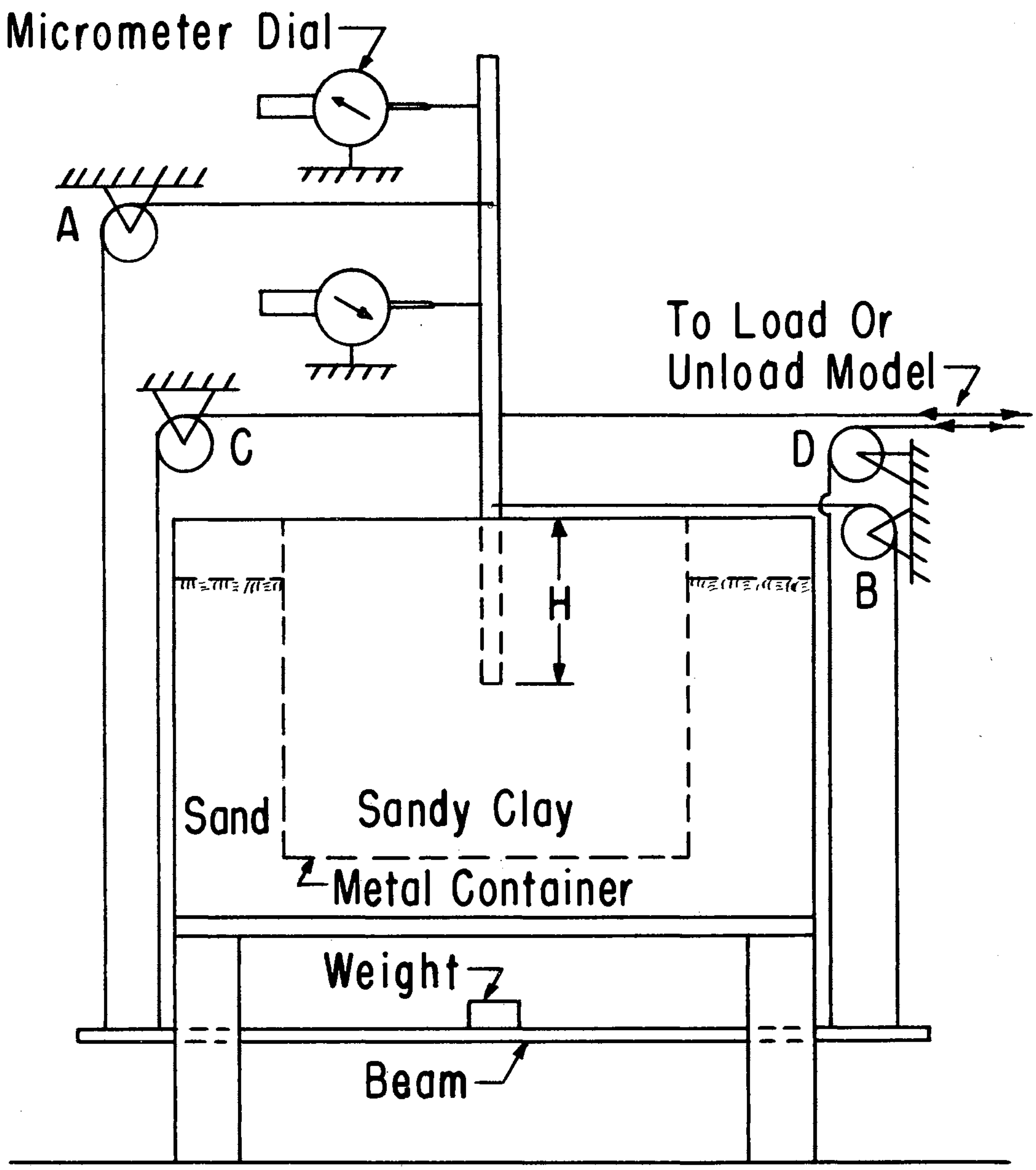

Figure 9. System Used for Loading Model Pier.

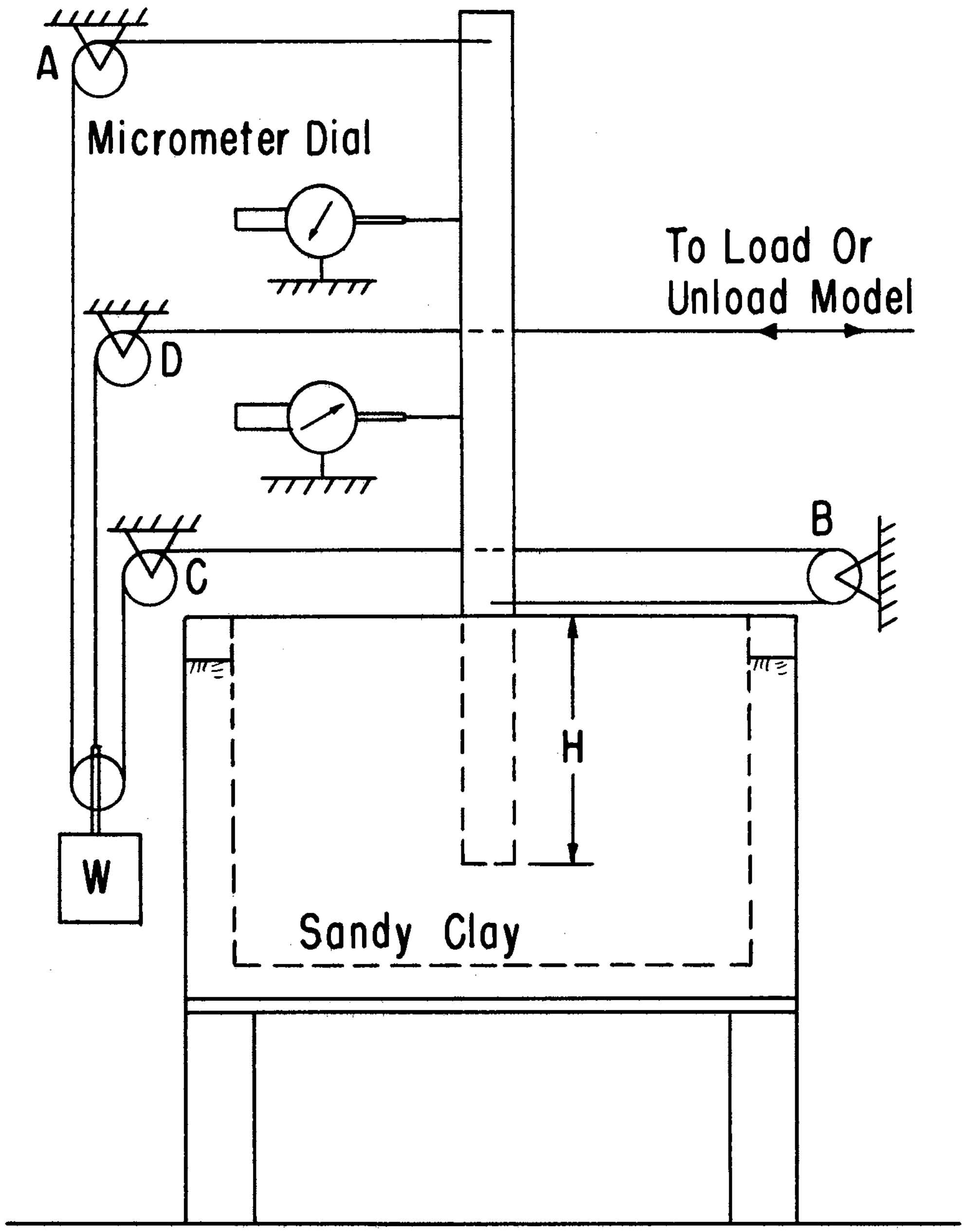

Figure 10. System Used for Loading Prototype Pier.

calculated. Five loading and unloading cycles were applied to all the piers except those in Test No. 4 where nine cycles were used. This test was used to determine the effect of repetitive loading.

Photographic Study

The sand was placed in the soil deformation visualization device as explained in Chapter IV. The pier was rotated from the vertical position to 18 degrees in increments of 2 degrees. Observations were made of the sand movements during the rotation of the pier. A photograph was made at the end of each increment.

CHAPTER VI

ANALYSIS OF DATA

Triaxial Test

The ratio of the applied stress to the confining pressure, σ_1/σ_3, was calculated for each increment of stress applied to the specimen. The corresponding strain, ε, was calculated by dividing the deformation in length by the original length.

The data for σ_1/σ_3 versus ε were plotted on log-log paper, as shown in Figures 11 and 12. Linear regression was used to determine the slope and intercept. A 95 per cent confidence interval was calculated for each curve. The confidence interval for each curve included the slopes of the other curves. Based on the analysis of the confidence intervals, it was hypothesized that the functions (curves) did not have different slopes.

The apparent cohesion of the soil was determined from the Mohr circles of stress, Figures 14 and 15. The apparent cohesion was 0.98 and 0.4 kilograms per square centimeter for the soil mixture containing 40 and 50 per cent clay, respectively.

A prediction equation for calculating the amount of strain that the soil containing 40 per cent clay and 9.5

per cent moisture undergoes in a triaxial test was derived by dimensional analysis.

The component equation for σ_1/σ_3 versus ε was:

$$\sigma_1/\sigma_3 = K\varepsilon^b = K\varepsilon^{.440} \qquad 6\text{-}1$$

where:

K = A constant

b = Slope

The average slope for the curves was used since the confidence intervals included the slope of all the curves.

To determine the relationship between C/σ_3 and ε, the intercepts at $\varepsilon = 1.0$ were plotted against the value of C/σ_3 for each confining pressure, as shown in Figure 13. The line of best fit was determined by the least squares method. The component equation for σ_1/σ_3 versus C/σ_3 was:

$$K = (\sigma_1/\sigma_3) = K_1(C/\sigma_3)^{.700} \qquad 6\text{-}2$$

Combining the component equation by multiplication and simplifying, the general prediction equation can be written as:

$$\varepsilon = [.100 \times \sigma_1/\sigma_3 \times 1/(C/\sigma_3)^{.700}]^{2.280} \qquad 6\text{-}3$$

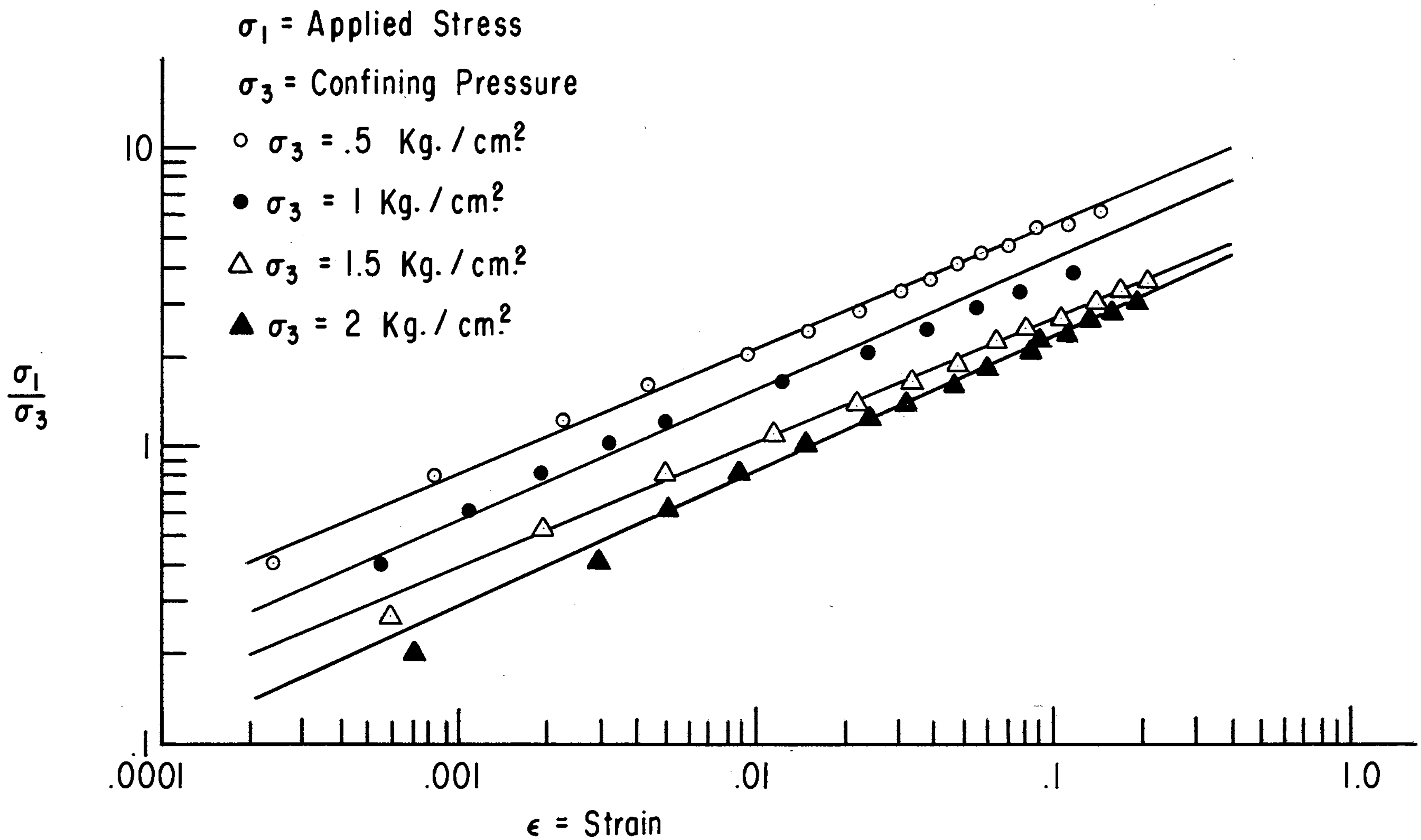

Figure 11. σ_1/σ_3 Versus ε for Triaxial Test on Soil Containing 40 Per Cent Clay.

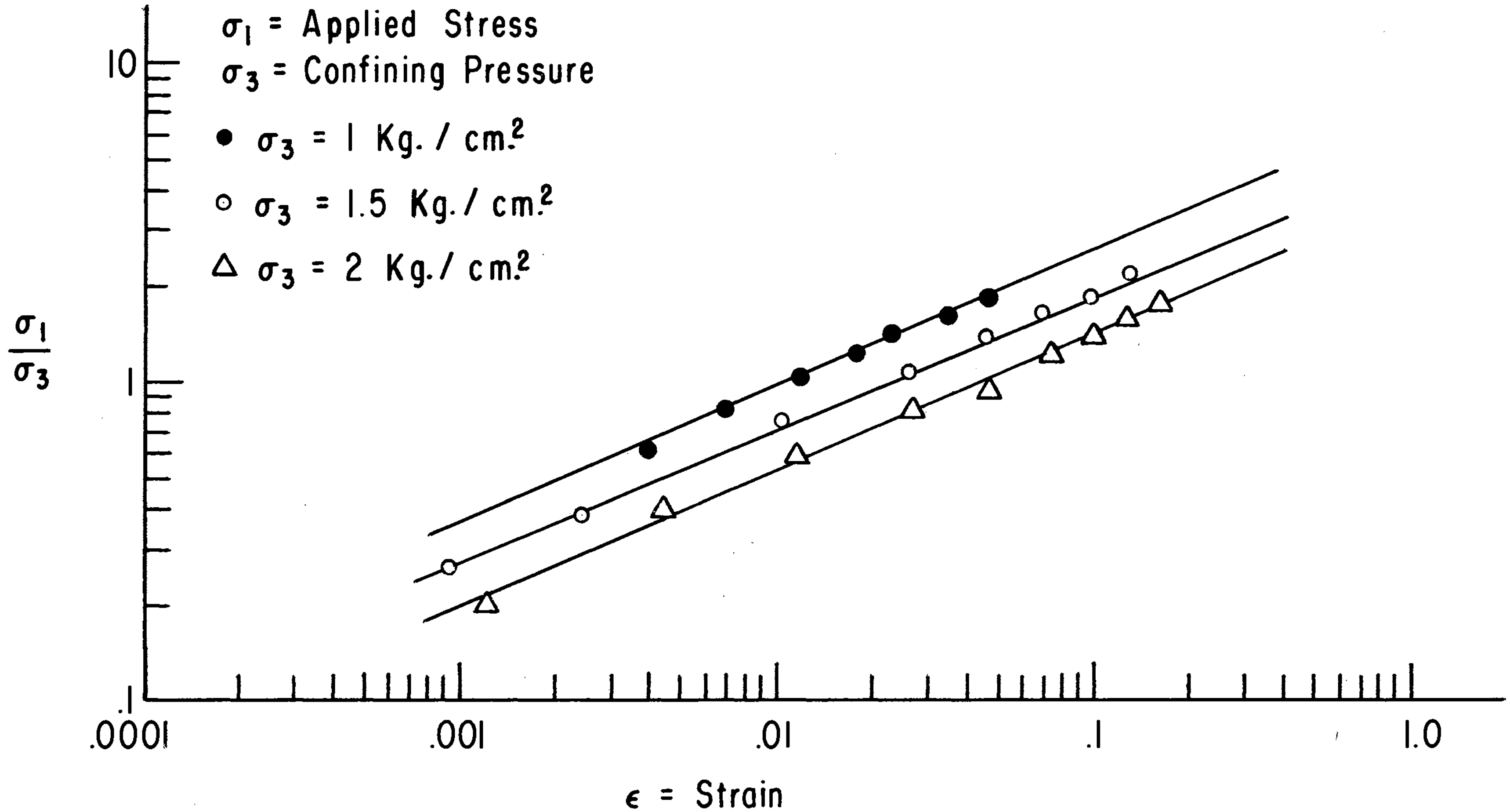

Figure 12. σ_1/σ_3 Versus ϵ for Triaxial Test on Soil Containing 50 Per Cent Clay.

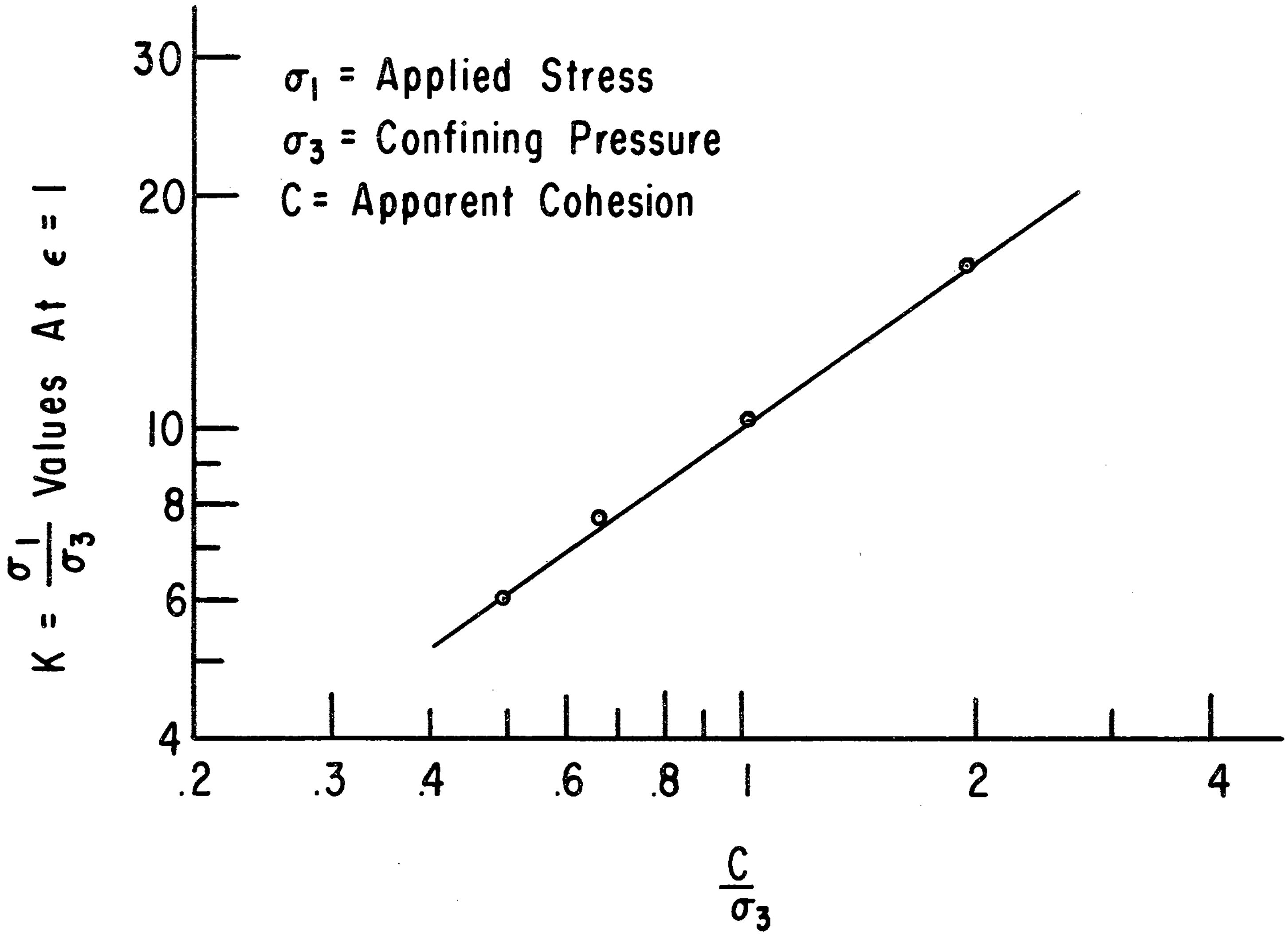

Figure 13. k Values Versus C/σ_3

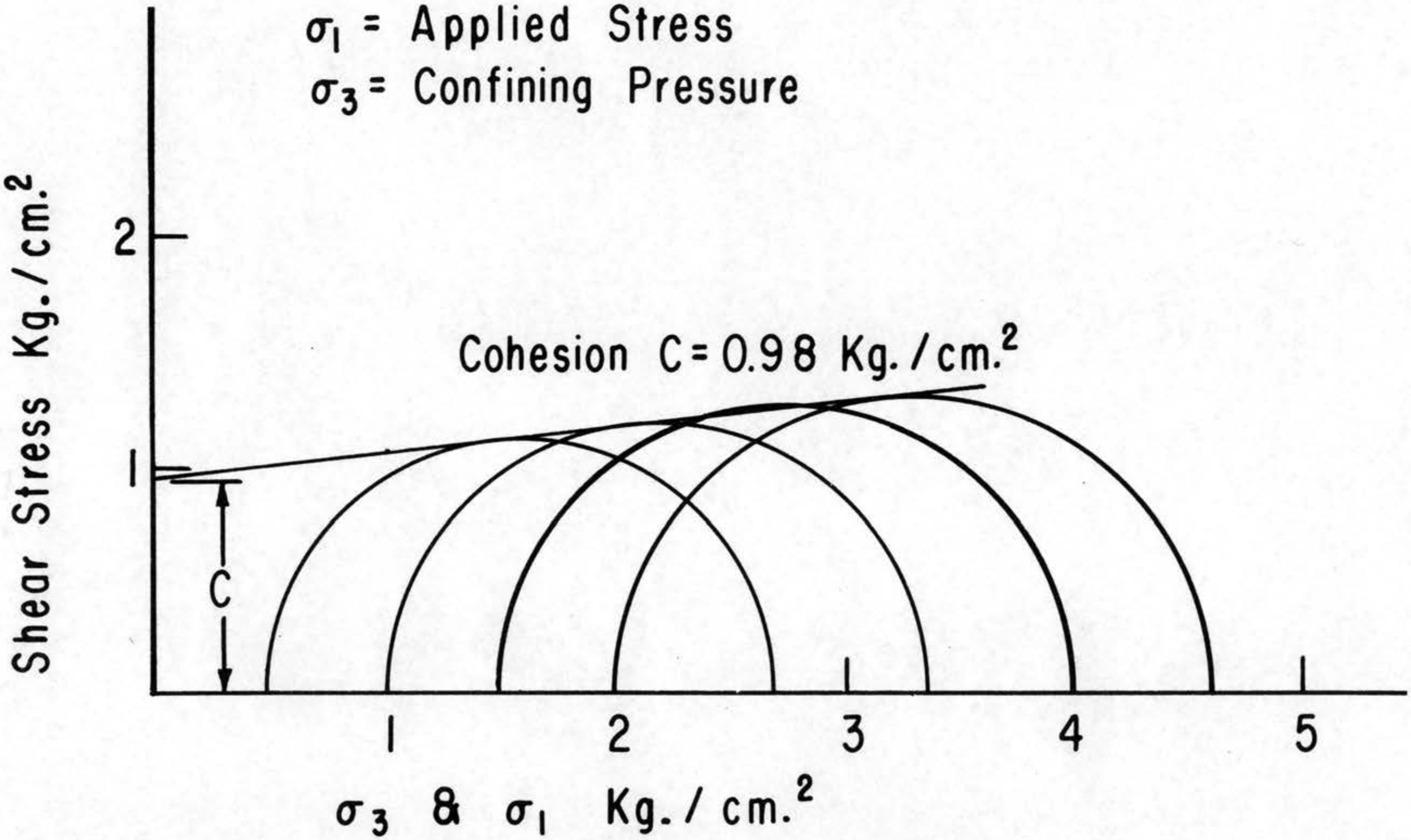

Figure 14. Consolidated-Undrained Triaxial Test on the Soil Containing 40 Per Cent Clay.

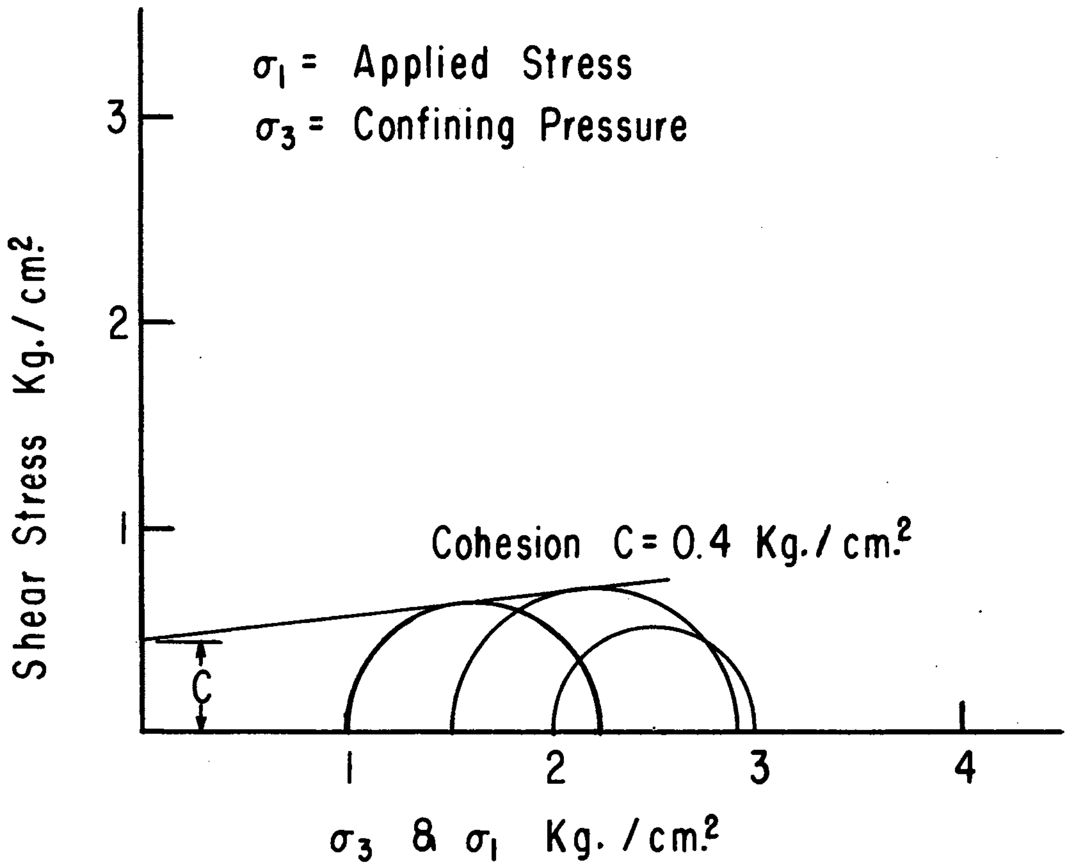

Figure 15. Consolidated-Undrained Triaxial Test on the Soil Containing 50 Per Cent Clay.

Model Pier Experiment

The initial analysis of the data consisted of plotting the data from the component equations on arithmetic, log-log and semi-log paper. The component equations for tan Θ versus H/D and tan Θ versus $M/G\rho DH^3$ indicated straight lines on log-log paper. It was hypothesized that these two component equations were of the form $y = ax^b$. A computer program using the least squares method was written to find the line of best fit for the data. The component equations and experimental data are shown in Figures 16 and 17.

The component equation for tan Θ versus H/D was:

$$\text{Tan } \Theta = .0002304\ (H/D)^{2.7318} \qquad 6\text{-}4$$

Correlation Coefficient (R) = .733

There was more variation in the data for this component equation as compared to the data for the other component equations. It is recognized that some variation can usually be expected in tests conducted with soils. This can be due to variation in such factors as density, permeability, moisture content, and thixotropy even though extreme care is exercised while conducting the test.

The component equation for tan Θ versus $M/G\rho DH^3$ was:

$$\text{Tan } \Theta = .01739\ (M/G\rho DH^3)^{2.3836} \qquad 6\text{-}5$$

R = .917

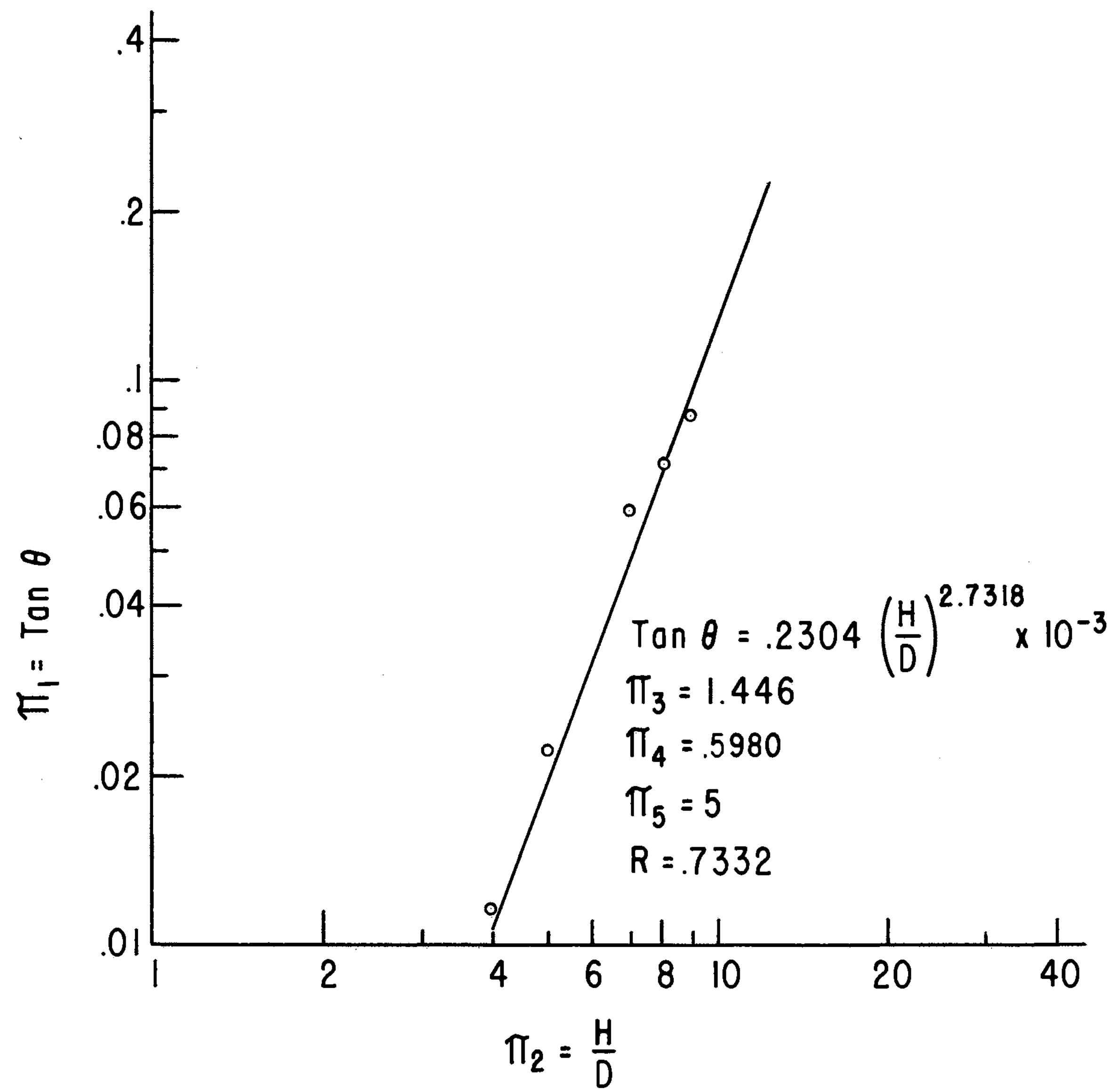

Figure 16. π_1 Versus π_2.

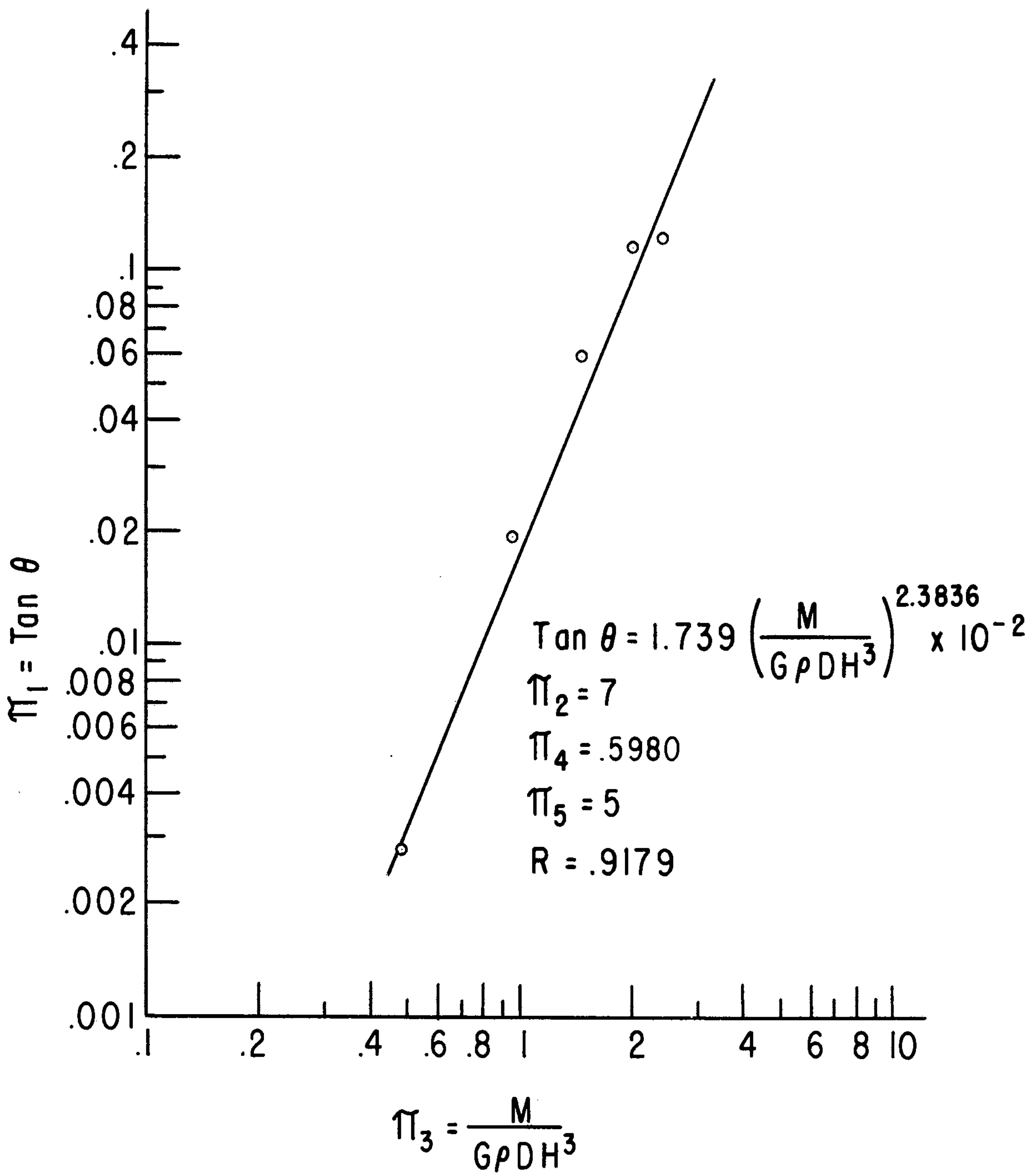

Figure 17. π_1 Versus π_3.

It was hypothesized that the component equation for tan Θ versus $KG\rho t/H$ which includes the time effect would approach an ultimate value if the pier were subjected to a given moment for an infinite length of time. To derive an equation by which the ultimate value of tan Θ could be determined, the data were transformed to give a straight line on arithmetic paper, Figure 18. The relationship between tan Θ and $KG\rho t/H$ could then be expressed by an equation of the form:

$$y = \frac{x}{a + bx} \qquad 6\text{-}6$$

where:

a = Intercept

b = Slope

The component equation for tan Θ versus $KG\rho t/H$ was:

$$\text{Tan } \Theta = \frac{KG\rho t/H}{.0115 + 16.7439\ KG\rho t/H} \qquad 6\text{-}7$$

The ultimate value of rotation can be obtained by taking the limit of the component equation as $KG\rho t/H$ becomes very large. The ultimate value of the equation is measured by the inverse of the slope, 1/b, of the straight line formed by the transformed data.

It was further hypothesized that the equation for tan Θ versus N would also approach an ultimate value as the number of loading and unloading cycles under a given moment approached infinity. The experimental data were transformed to give

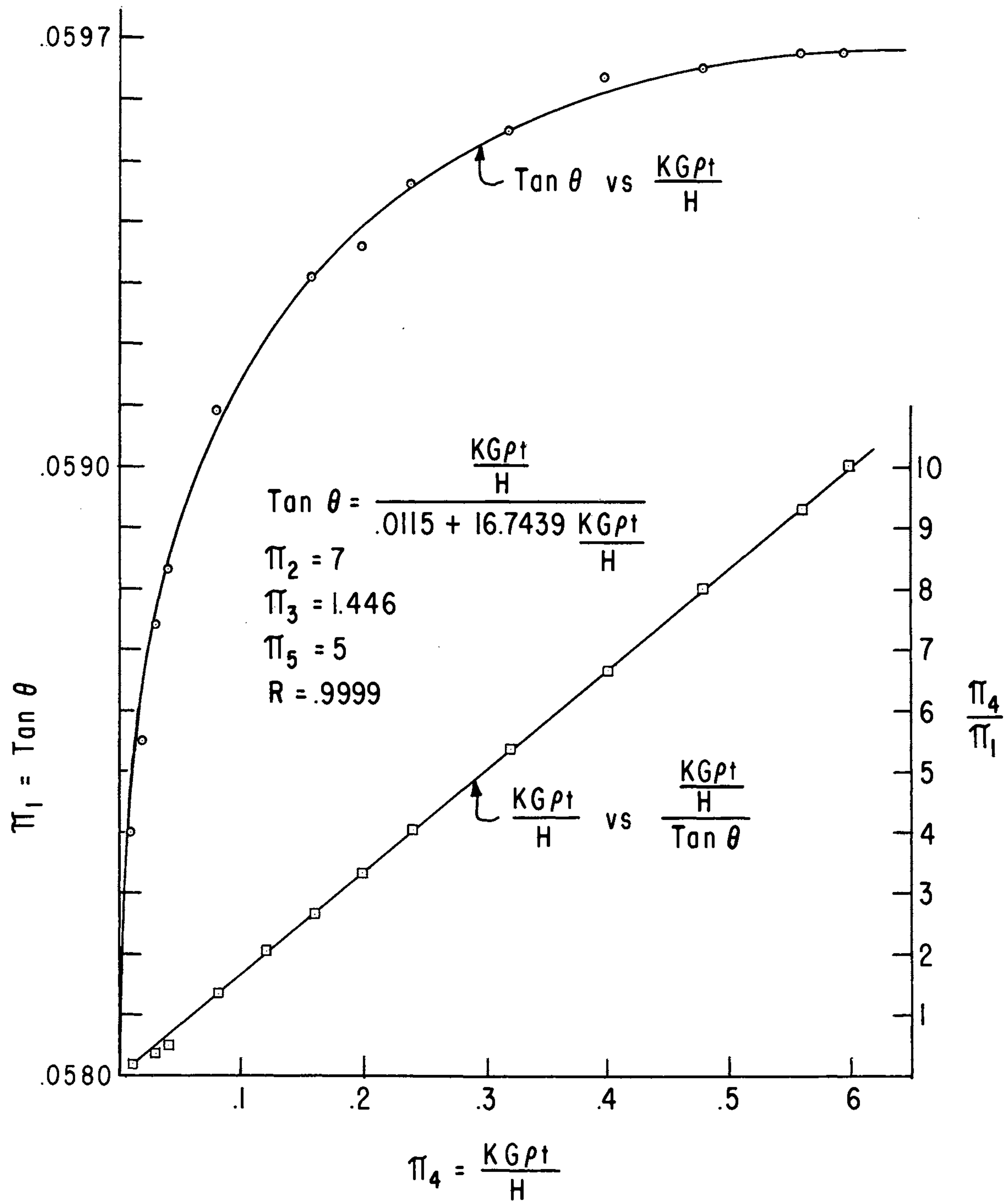

Figure 18. π_1 Versus π_4.

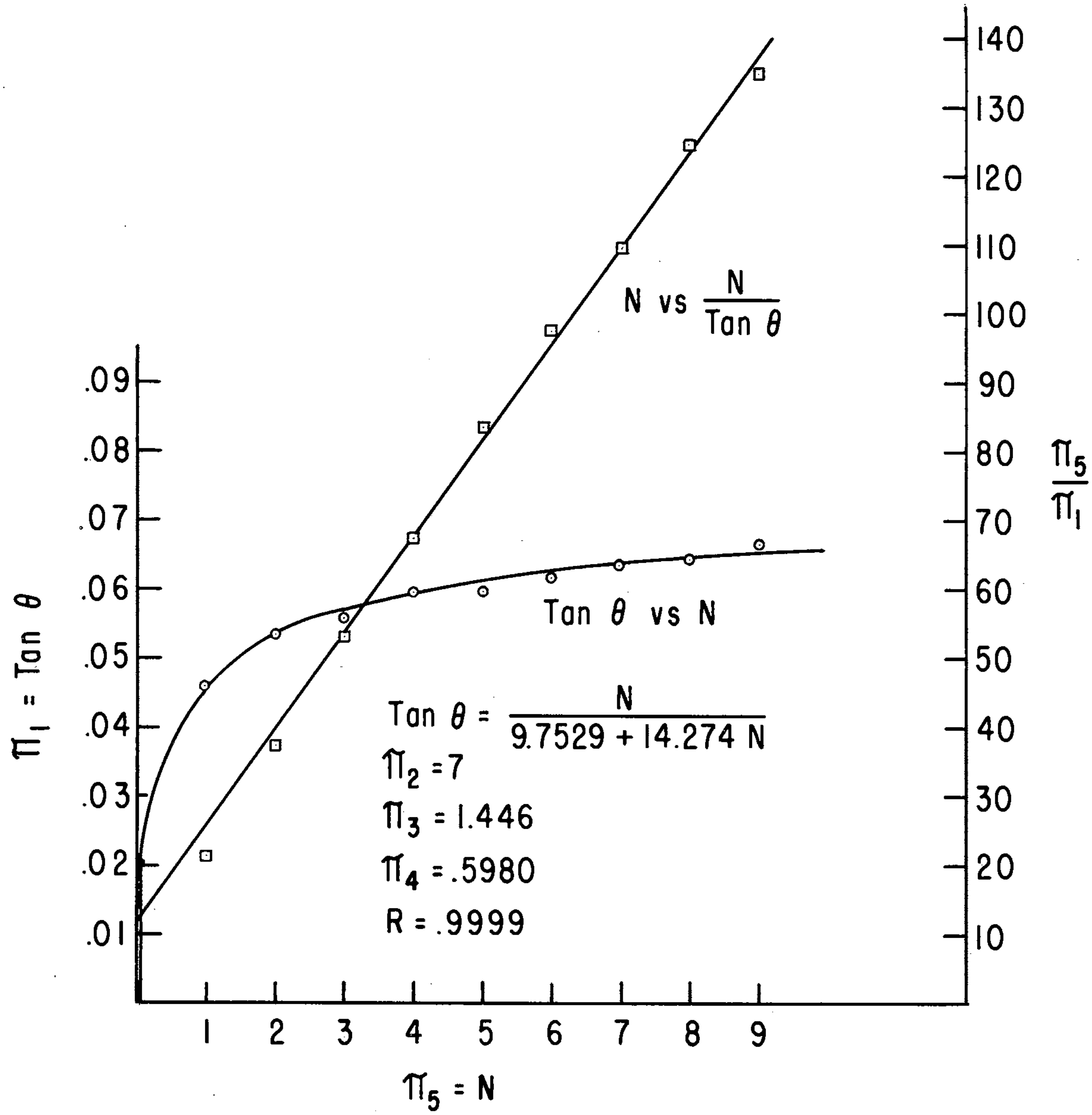

Figure 19. π_1 Versus π_5.

a straight line on arithmetic paper as above and is shown in Figure 19. The component equation for this relationship was:

$$\text{Tan } \Theta = \frac{N}{9.7529 + 14.2740\ N} \qquad 6\text{-}8$$

Since the experimental data for tan Θ versus H/D and tan Θ versus $M/G\rho DH^3$, and the transformed data for tan Θ versus $KG\rho t/H$ and tan Θ versus N indicate straight lines on log-log paper, the component equations can be combined by multiplication to form the general prediction equation.

$$\text{Tan } \Theta = C[.0002304\ (\pi_2)^{2.7318} \times .01739\ (\pi_3)^{2.3836} \times \pi_4/(.0115 + 16.7439\ \pi_4) \times \pi_5/(9.7529 + 14.274\ \pi_5)] \qquad 6\text{-}9$$

The value of the constant C for the general prediction equation was determined by taking the average of the constants as determined by the proper component equation for all the tests. This method allowed each test to contribute to the value of the constant in the prediction equation. The value of the constant was found to be 6783.

Substituting the value of the constant into the general equation and simplifying, the prediction equation becomes:

$$\text{Tan } \Theta = .02718\ [(\pi_2)^{2.7318} \times (\pi_3)^{2.3836} \times \pi_4/(.0115 + 16.7439\ \pi_4) \times \pi_5/(9.7529 + 14.274\ \pi_5)] \qquad 6\text{-}10$$

It must be noted that this equation is valid only for piers having the same geometrical configuration and where soil properties are such that the pi terms are within the ranges used for the present experiments and analysis.

CHAPTER VII

DISCUSSION AND APPLICATION OF RESULTS

Triaxial Tests

The exponents in the component Equation 6-1 and 6-2 are the slopes of the regression lines for the experimental data of σ_1/σ_3 versus ε and σ_1/σ_3 versus C/σ_3. They are indices of the strength property of the soil when subjected to an applied stress and a confining pressure. The slopes of the regression lines can be designated as the strength indices of the soil specimens. The prediction equation derived from the data from these tests has shown that the deformation of a confined soil can be characterized by one strength property, the confining pressure, and the applied stress.

The specimen began to bulge at approximately 0.06 inch/inch strain. It was assumed that the specimens had failed at 0.1 inch/inch strain. The stresses at 0.1 inch/inch strain were used in drawing the Mohr circles of stress.

Figure 20 shows a specimen after a test had been completed. The bulging all around the specimen was typical for most of the specimens tested.

For the same value of σ_1/σ_3 the strain was greater for the soil mixture containing 50 per cent clay. This would be expected since soils containing the larger fraction of clay will tend to deform more.

Model and Prototype Pier Experiment

A comparison of the observed values and the predicted values for tan Θ for the model piers is shown in Figure 21. One point in each loading cycle was selected at random for comparison. If there had been perfect agreement in the observed and predicted values, all of the points would be located on the 45 degree line. An analysis to determine the line of best fit for the data yielded a slope of 0.984 for the regression line and a correlation coefficient of 0.954. The slope of the regression line being less than one indicates that the values obtained by the prediction equation were a little larger than the observed values.

A comparison of the observed values and the predicted values for tan Θ for the prototype pier is shown in Figure 22. The predicted values were determined with the equation derived for the model piers. An analysis of the data yielded a slope of 1.15 and a correlation coefficient of 0.967. Eighty-four per cent of the predicted values deviated ± 20 per cent or less from the observed values.

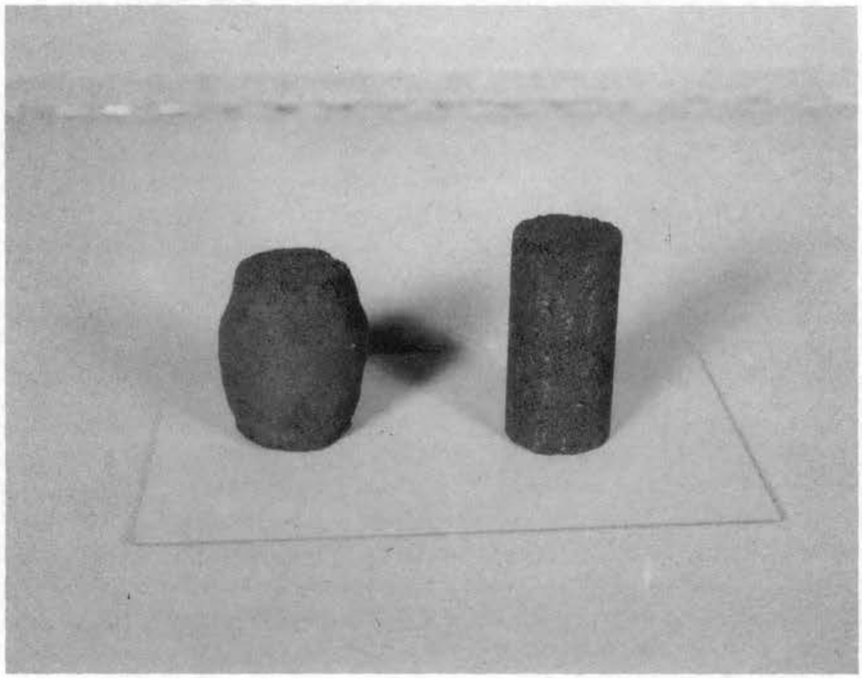

Figure 20. Soil Specimen After and Before Testing.

Application of Prediction Equation

An equation that can be used for predicting the rotation of a pier foundation would have many applications in the design of rigid or pole-type structures. There is a limit to the amount of movement a structure can undergo without causing damage to the structure. To design an adequate foundation, the designer should be able to predict the amount of rotation that will occur.

The prediction equation developed in this study can be used to determine how the rotation of a pier is effected by the depth of embedment, pier diameter, soil density, soil permeability, repetitions of loadings, and elapsed time of loading.

The equation could also be used for the design of foundations for supports for signs across highways, utility poles, and guardrails along highways.

Some examples of the applications of the equation for predicting the rotation of a pier are shown in Figures 23, 24, 25, and 26. The calculations are based on the moment produced by the wind load acting on the side of a pole structure with a wall height of 14 feet, a 1:3 roof slope, and a pole spacing of 15 feet center to center along the wall. Using the recommended 20 pounds per square foot design load, it was calculated that the moment acting on one pole would be approximately 13,064 foot-pounds. The amount of rotation

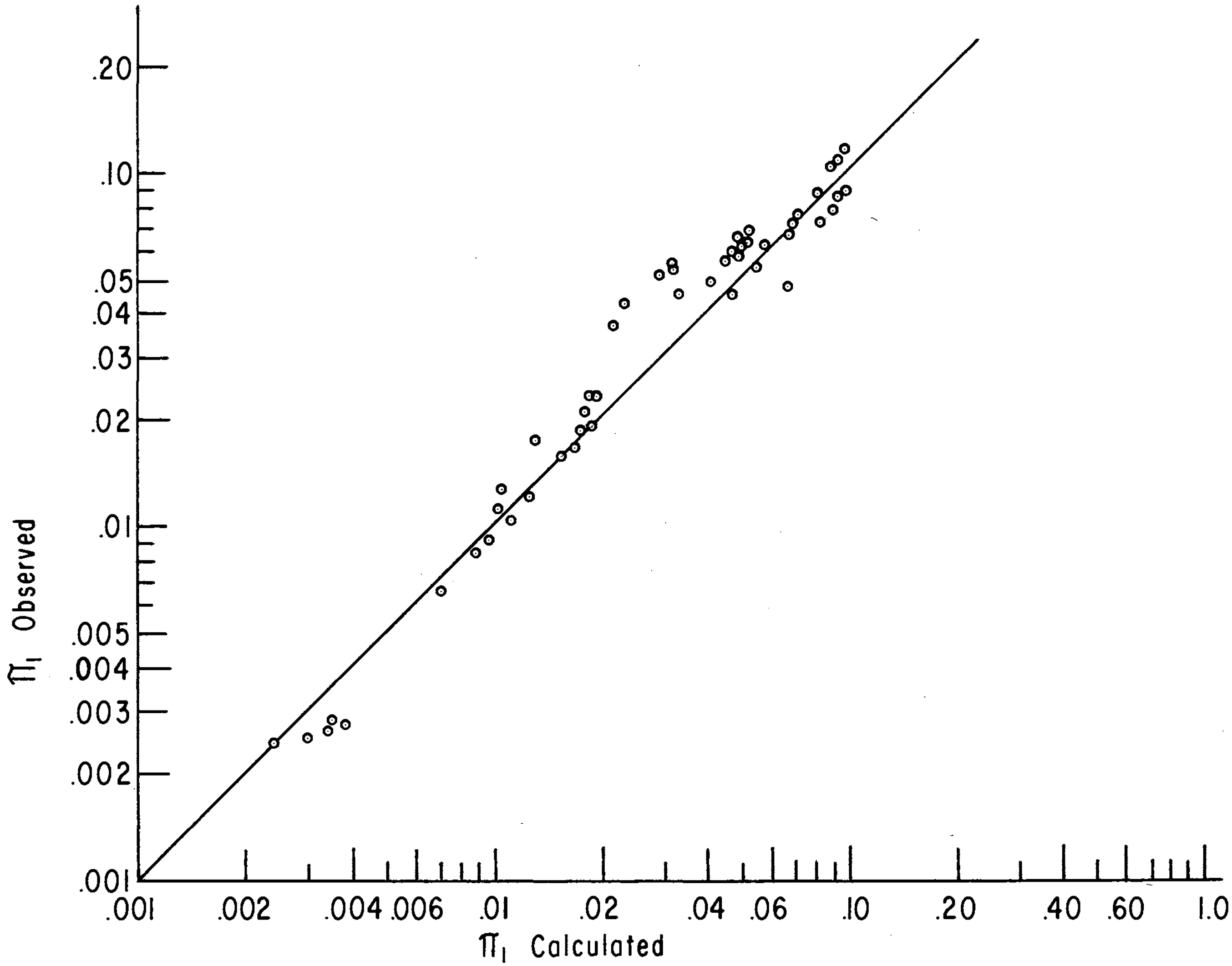

Figure 21. π_1 Calculated Versus π_1 Observed for Model.

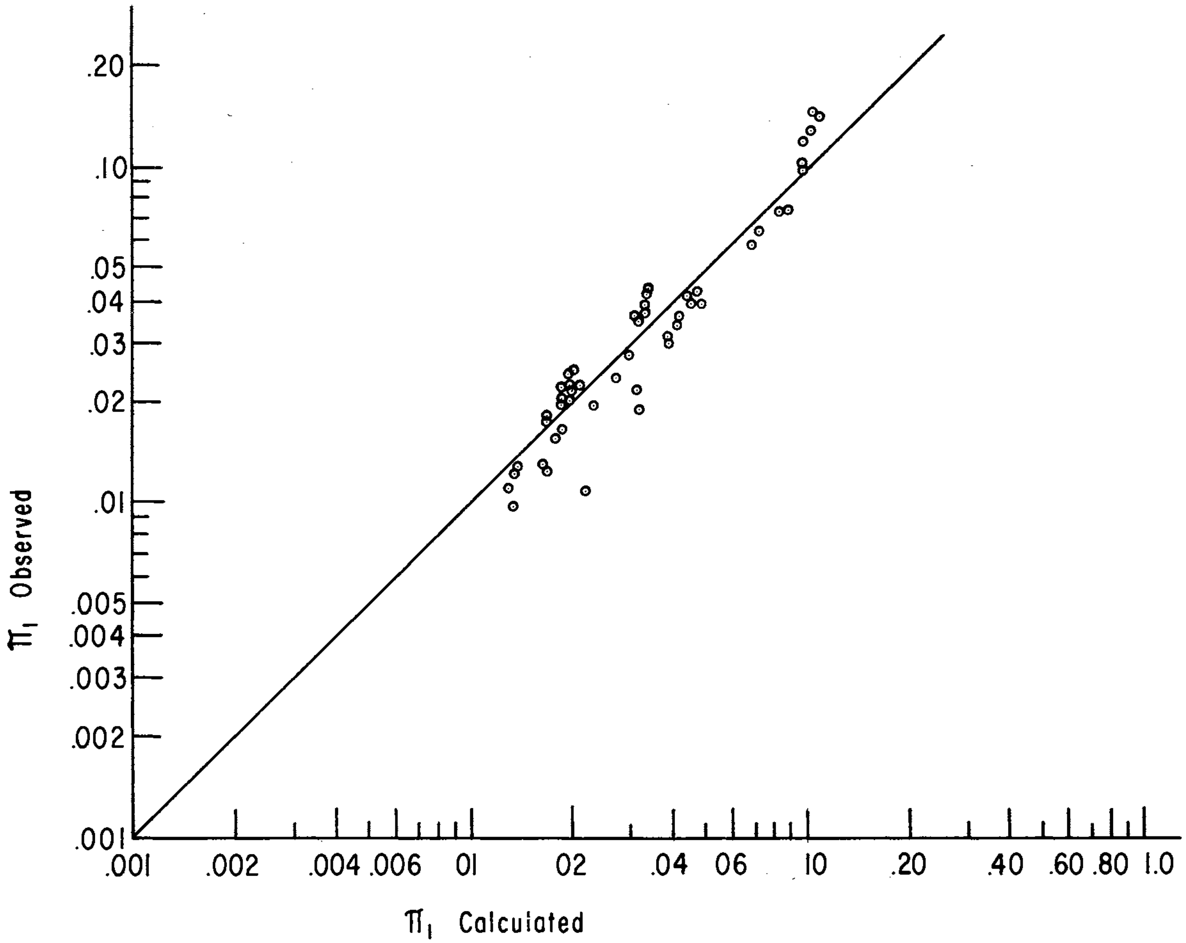

Figure 22. π_1 Calculated Versus π_1 Observed for Prototype.

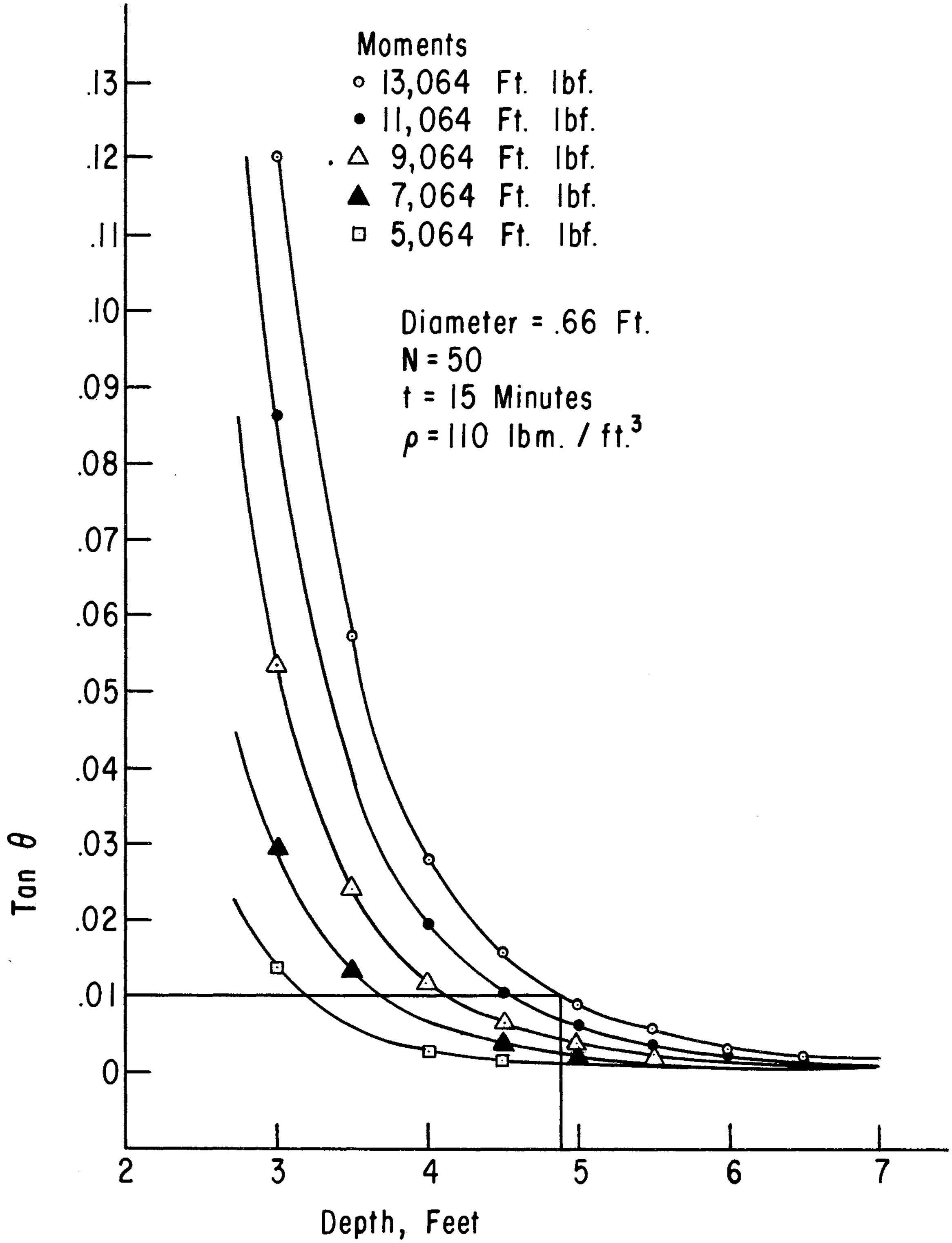

Figure 23. Tan θ Versus Depth of Pier.

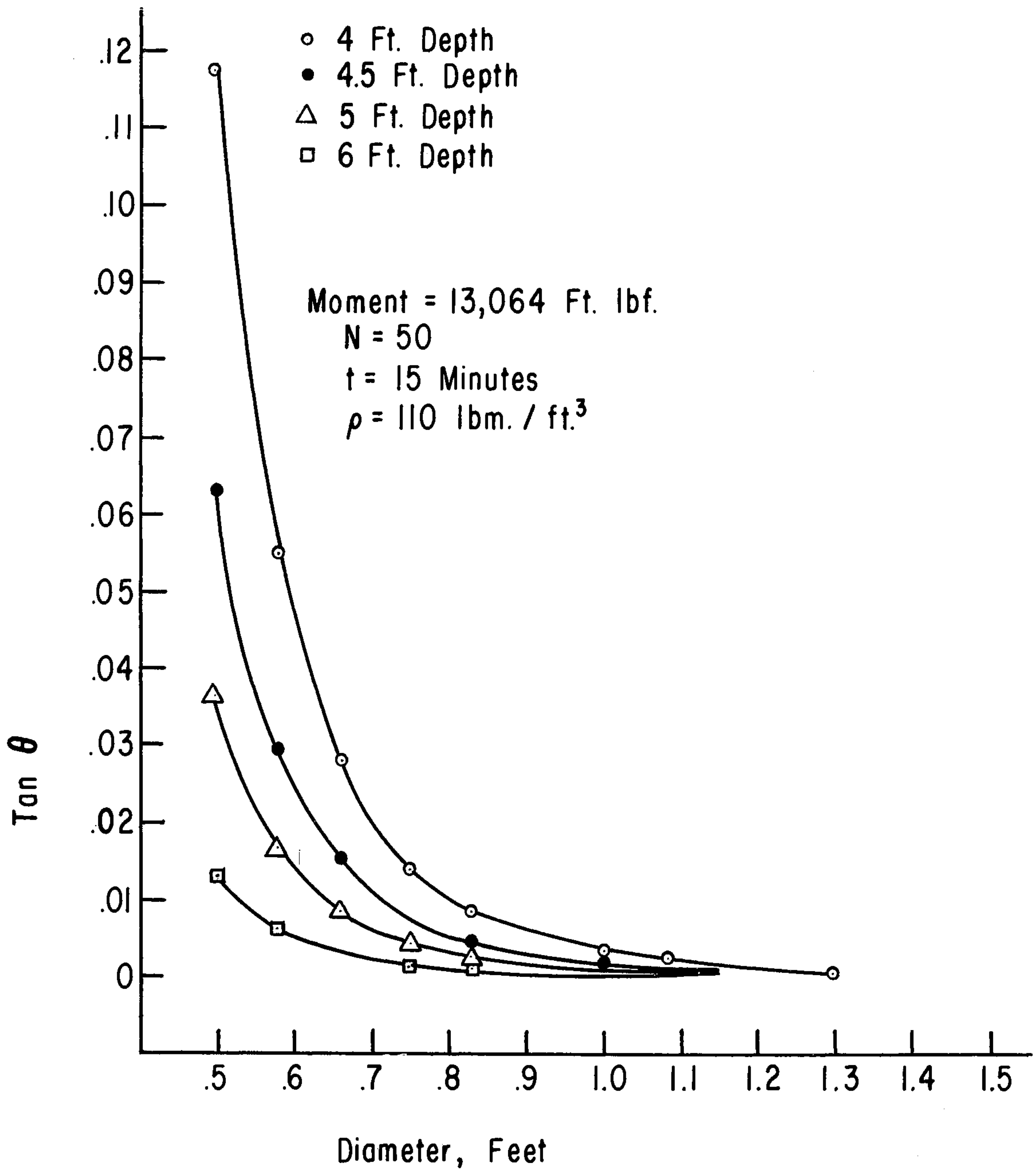

Figure 24. Tan θ Versus Diameter of Pier.

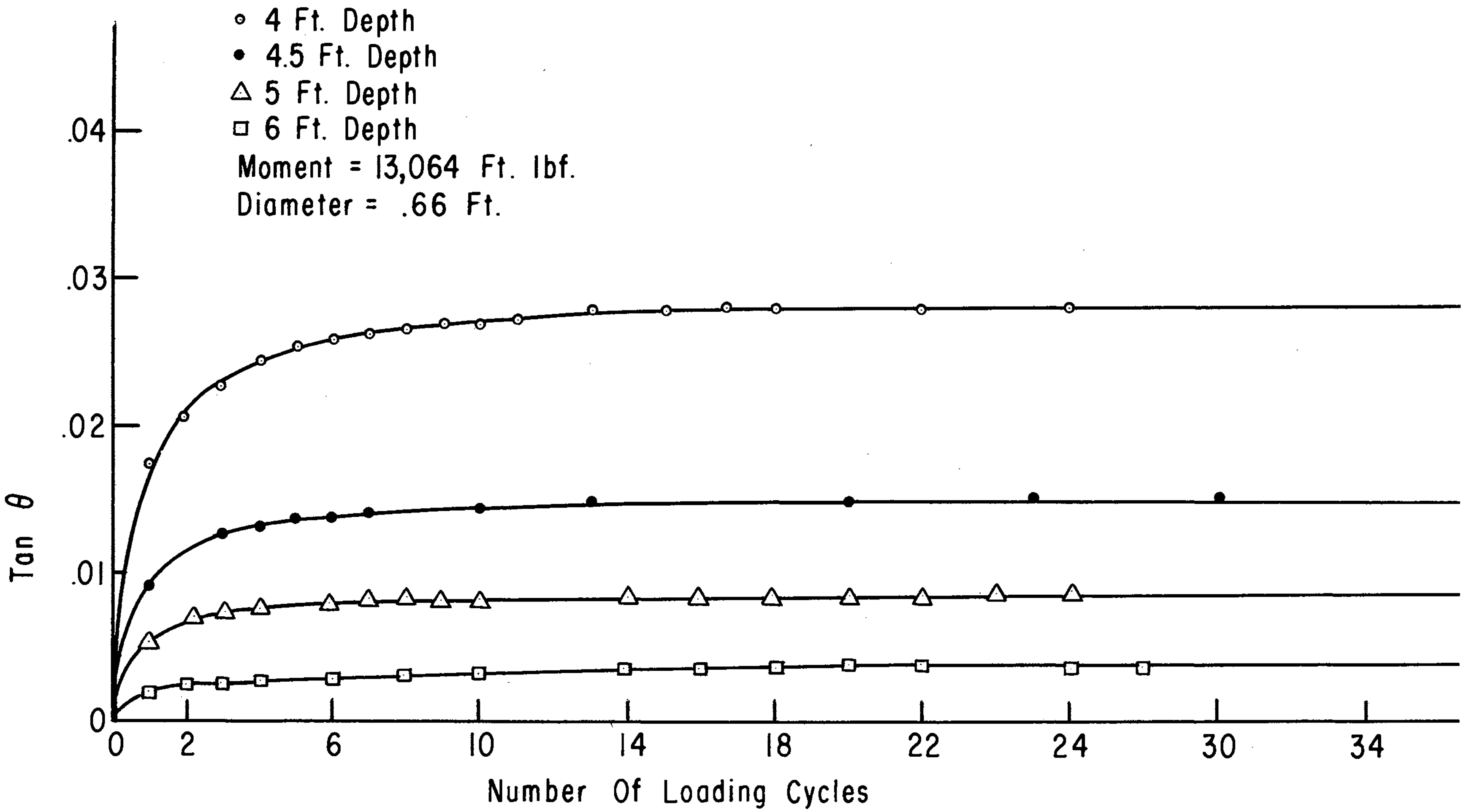

Figure 25. Tan θ Versus Number of Loading Cycles.

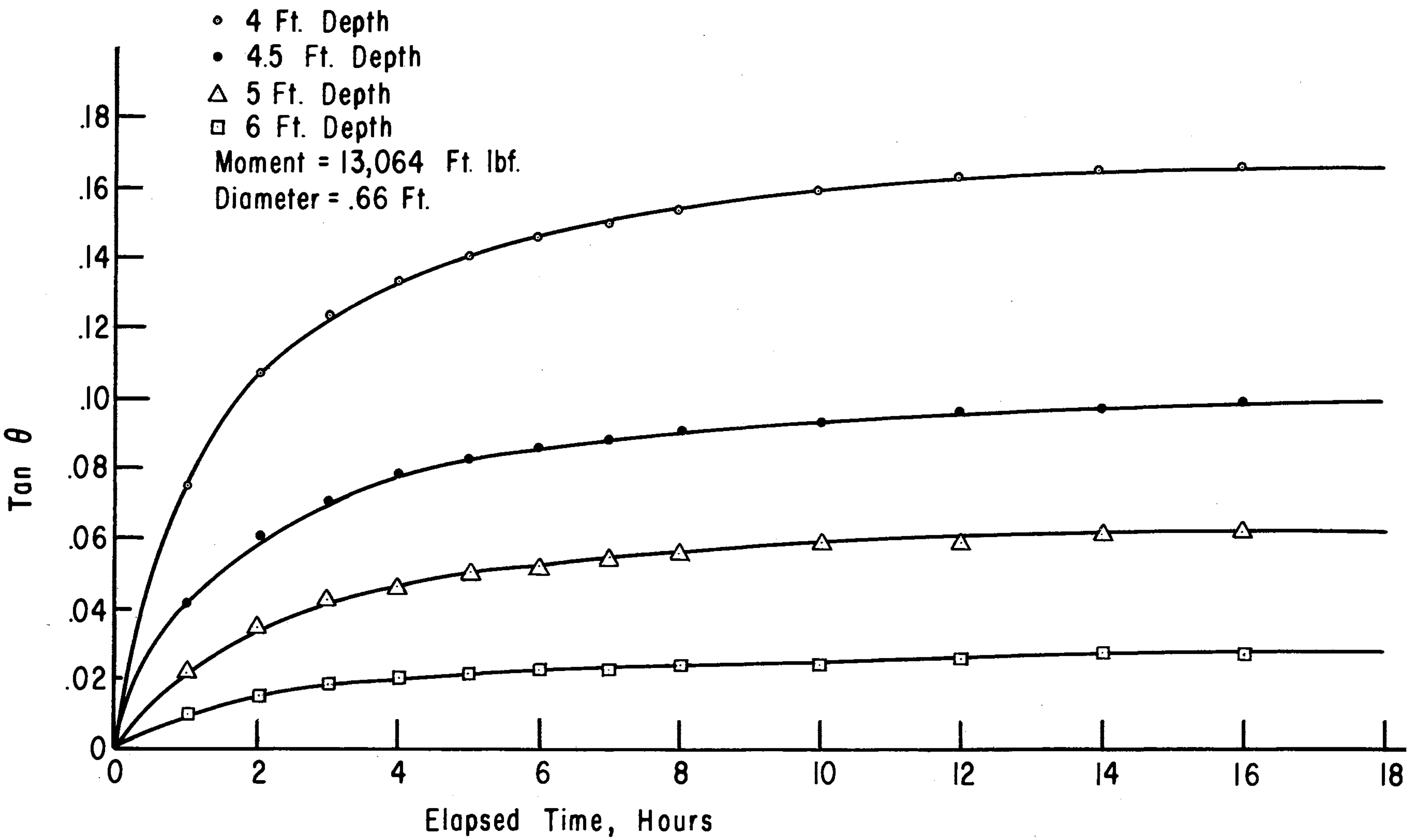

Figure 26. Tan θ Versus Elapsed Time.

that this moment will cause on piers 8 inches in diameter and embedded at different depths is shown in Figure 23. The amount of rotation caused by smaller moments is also shown.

The required depth necessary to limit the rotation of an 8-inch pier to a certain value can be determined from these graphs. Suppose that a moment of 13,064 foot-pounds is acting on a pier and it is desired to limit the rotation to $\tan \theta = 0.01$. Drawing a line horizontally from $\tan \theta = 0.01$ to intersect the graph for the 13,064 moment gives an embedment depth of 4.9 or 5 feet.

The graphs in Figure 24, 25, and 26, show the relationship of the rotation of the piers to the diameter of the pier, number of loading cycles, and elapsed time of loading. These relationships can be used in the same manner as explained above.

Behavior of Clay Soil

The deformation of the clay soil used in the experiment was similar to the deformation of the sand used in the photographic study discussed in the next section. The soil in front of the pier would begin bulging upward as the pier rotated. The size of the bulging area increased as the rotation increased. The bulging area was probably the zone of soil that had undergone failure during the rotation of the pier. It appeared that the failure zone never extended more than three pier diameters from the pier in the direction of rotation.

Photographic Study

A soil deformation visualization device was constructed to study the soil deformation developed by a rotating pier. A rectangular pier was embedded at the side of a clear plastic box filled with Ottawa sand. A one-inch grid was constructed with black sand adjacent to the side of the box. The development of the deformed zone is shown in sequence in Figures 27 through 32.

It was observed that the sand in front of the pier began bulging upward immediately after rotation began, Figure 28. As rotation continued, the height and length of the bulging area increased. It appeared that a very thin layer of sand along the surface failed by shear at the beginning of rotation and the failure zone progressed outward and downward as rotation increased, Figure 29. The deformed zone in front of the pier below the surface did not extend more than three pier widths out from the pier as can be observed by the undistorted grid lines, Figure 32. There is also a smaller deformed zone back of the pier at the bottom. There appeared to be little or no deformation in a vertical direction below the bottom of the pier, Figure 32. As the pier moved away from a zone, the space previously occupied by the pier was immediately filled by sand flowing downward into it, Figure 32.

The pier was pinned tightly to the side of the box at a distance two-thirds of the embedded depth below the surface. This was necessary to try to prevent sand from flowing between the pier and the side of the box.

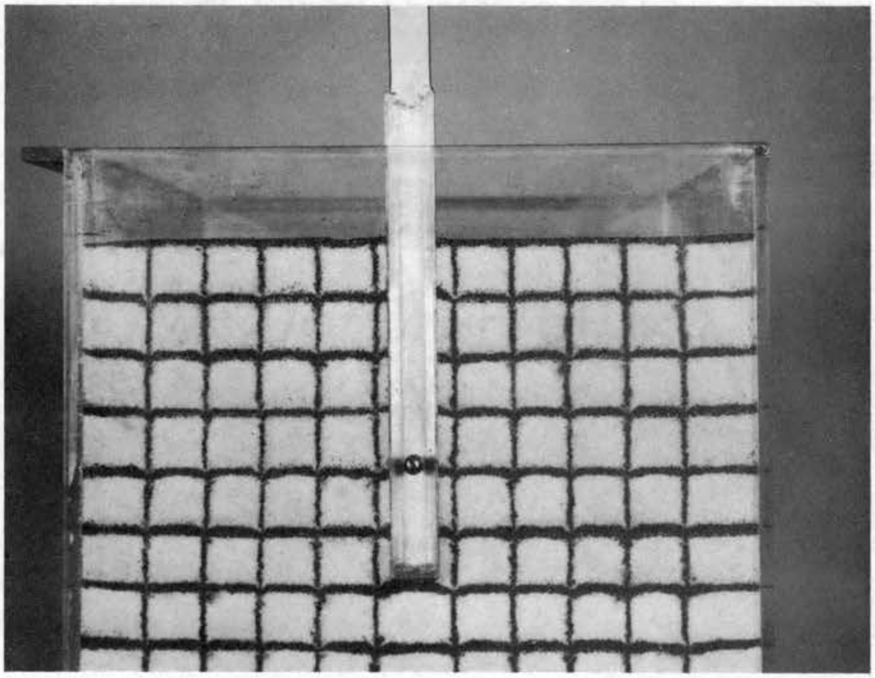

Figure 27. Initial Position of Pier.

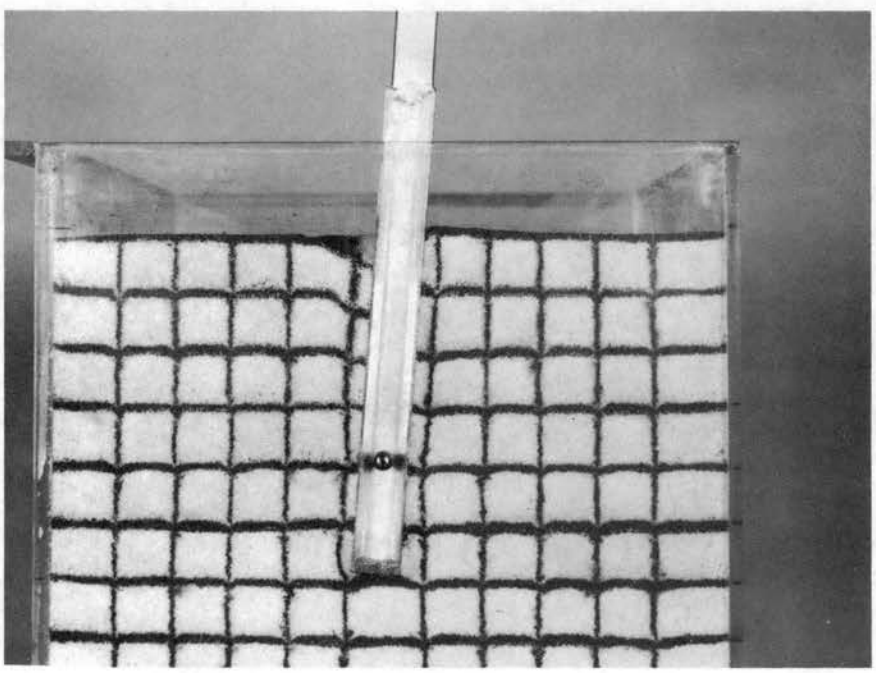

Figure 28. Four Degrees Rotation.

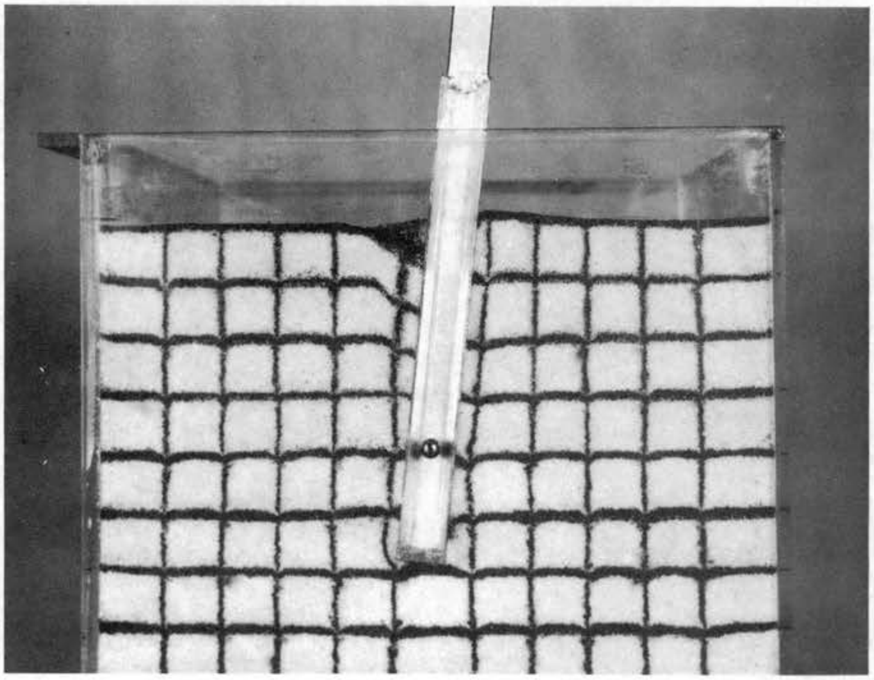

Figure 29. Six Degrees Rotation.

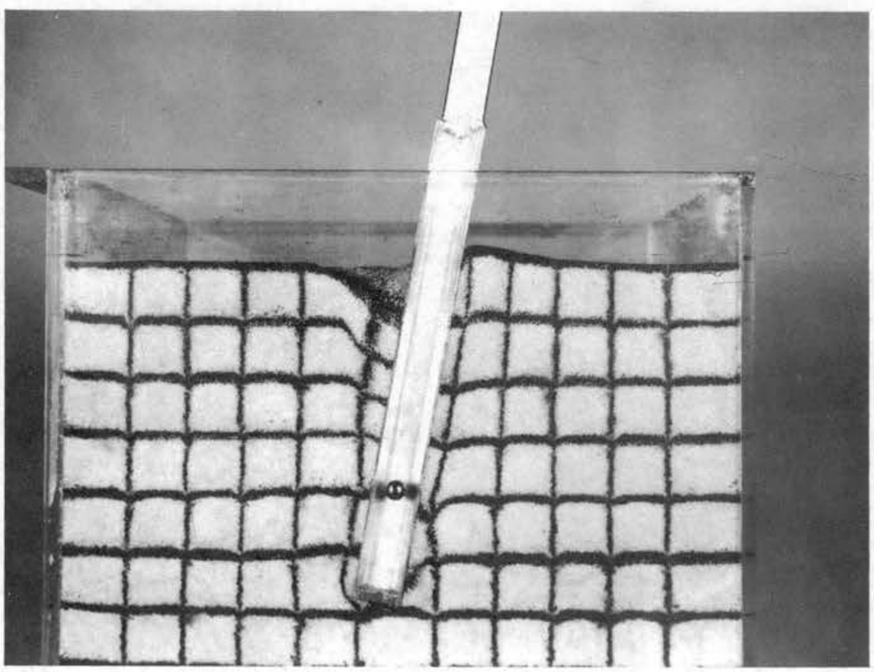

Figure 30. Ten Degrees Rotation.

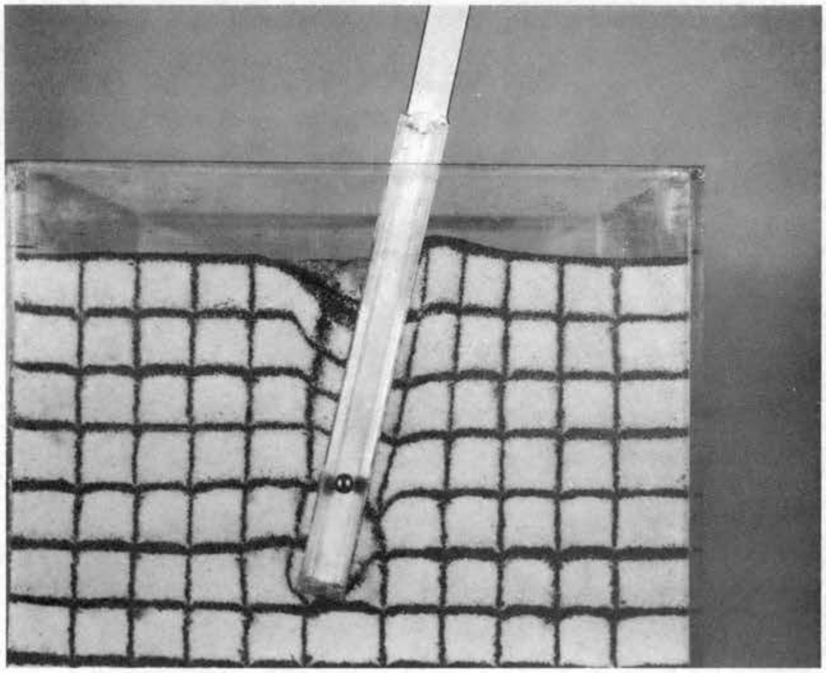

Figure 31. Twelve Degrees Rotation.

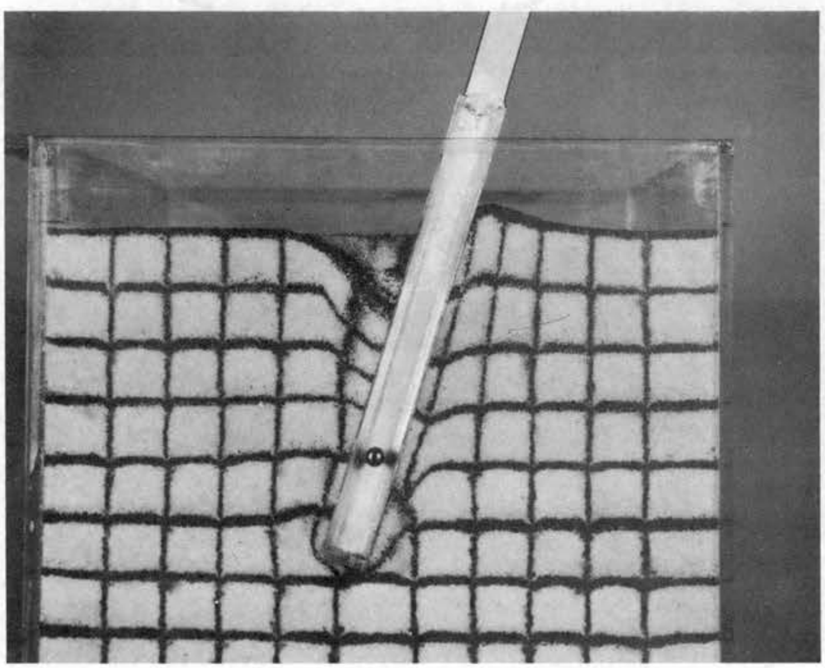

Figure 32. Sixteen Degrees Rotation.

CHAPTER VIII

SUMMARY AND CONCLUSIONS

Summary

The objectives of this study were:

1. To develop a prediction equation for determining the rotation of shallow pier foundations subjected to an overturning moment.
2. To validate the equation with data obtained in the laboratory with a prototype.
3. To determine the effect of repetitive loading on the rotation of shallow pier foundations.

The principles of dimensional analysis and similitude were employed to facilitate the research. By using dimensional analysis and similitude, the number of variables could be reduced by combining the pertinent quantities into dimensionless groups fewer in number than the original set of quantities.

The dimensionless ratios used in the experiment were:

$\pi_1 = \theta$

$\pi_2 = H/D$

$\pi_3 = M/G\rho DH^3$

$\pi_4 = KG\rho t/H$

$\pi_5 = N$

π_1 was designated as the dependent variable. The other four pi terms were treated as independent variables.

The experiment was conducted in the laboratory using a saturated mixture of Ottawa sand and Permian clay. The test schedule as shown in Table III was followed so that the experimental data could be used to develop a prediction equation of the form:

$$\pi_1 = f(\pi_2, \pi_3, \pi_4, \pi_5) \qquad 8\text{-}1$$

The component equations relating the dependent variable to each independent variable were developed by using the least squares method. The component equations were:

$$\text{Tan } \Theta = .0002304\ (H/D)^{2.7318} \qquad 8\text{-}2$$

$$\text{Tan } \Theta = .01739\ (M/G\rho DH^3)^{2.3836} \qquad 8\text{-}3$$

$$\text{Tan } \Theta = \frac{KG\rho t/H}{.0115 + 16.7439\ KG\rho t/H} \qquad 8\text{-}4$$

$$\text{Tan } \Theta = \frac{N}{9.7529 + 14.2740\ N} \qquad 8\text{-}5$$

The experimental data for the component equations tan Θ versus H/D and tan Θ versus $M/G\rho DH^3$, and the transformed data for tan Θ versus $KG\rho t/H$ and tan Θ versus N indicated straight lines on log-log paper; therefore, the equations could be combined by multiplication to form the prediction equation.

The regression lines for the observed values versus predicted values yielded a slope of 0.984 and a correlation coefficient of 0.954 for the models, and a slope of 1.15 and a correlation coefficient of 0.966 for the prototype.

The confidence intervals for the curves for the data from the triaxial test indicated that all the curves had the same slope.

Conclusions

1. The deformation of soil confined in a direction normal to the applied load can be adequately characterized by one strength property, as long as the coefficient of friction does not change.

2. The strain of the soil subjected to an applied stress and confining pressure can be predicted by the following prediction equation:

$$\varepsilon = [.100 \times \sigma_1/\sigma_3 \times 1/(C/\sigma_3)^{.700}]^{2.280}$$

This equation is valid only where the conditions are such that the pi terms are within the range used for the present experiment and analysis.

3. The rotation of an embedded pier may be described by a prediction equation of the form:

$$\text{Tan}\ \Theta = .02718\ [(\pi_2)^{2.7318} \times (\pi_3)^{2.3836} \times \pi_4/(.0115 + 16.7439\ \pi_4) \times \pi_5/(9.7529 + 14.274\ \pi_5)]$$

It must be noted that the prediction equation is valid only where the conditions are such that the pi terms are within the range used for the present experiment and analysis.

4. The rotation under a given moment appears to reach an ultimate value as the length of time the pier is subjected to a given moment increases. For an 8-inch pier embedded 5 feet and subjected to a 13,064 foot-pounds moment, the rotation would reach 90 per cent of the ultimate value in approximately 14 hours.

5. For a constant moment, the effect of repetitive loading decreases as the number of loading cycles increases.

For the prototype conditions given in 4 above, the effect of repetitive loading would be very small after 50 loading cycles.

Suggestions for Further Study

1. Develop prediction equations which would include the additional effect of different moisture content of the soil, and different soil properties such as cohesive strength and internal friction angle.

2. Determine the behavior of a pier subjected to a couple and horizontal shear.

3. Conduct an experiment using piers equipped with strain gauges to determine how bending interacts with soil pressure variation, and hence rotation.

4. Validate the prediction equation with full-size prototype.

BIBLIOGRAPHY

1. Abbett, R. W. "Stability of Cantilever Poles in Sandy Soil." Civil Engineering, Vol. 11, pp. 301-303, Discussion p. 434, 1941.

2. Anderson, W. C. "Pole Foundations to Resist Tilting Moments." Electric Light and Power, XXVI, 96, October, 1948.

3. Anderson, W. C. "Foundation to Resist Tilting Moments Imposed on Upright Cantilevers Supporting Highway Signs." Highway Research Board, Bulletin 247, p. 1, 1960.

4. Appleford, C. W. "Method of Handling the Problem of Pole Embedment." Civil Engineering, Vol. 5, p. 311, 1935.

5. Beckett, F. E. "An Experiment Study of Model Poles Under Lateral Loads." Unpublished thesis on file at the Oklahoma State University Library. Stillwater, 1958.

6. Behn, F. E. "Tests of Tilting Moment Resistance of Cylindrical Reinforced Concrete Foundations for Overhead Sign Supports." Highway Research Board, Bulletin 247, p. 14, 1959.

7. Browne, W. H., Jr. and J. Fontaine. "Tests of North Carolina Poles for Electrical Distribution Lines." North Carolina State College of Agricultural and Engineering Experiment Station Bulletin No. 3, 1929.

8. Chung. T. J. "Analysis of Cohesive and Frictional Resistance of Soil as Related to the Geometrical Configuration of the Particles." Unpublished thesis on file at the Oklahoma State University Library. Stillwater, Oklahoma, 1965.

9. Czerniak, E. "Resistance to Overturning of Single Short Piles." Proceedings of the American Society of Civil Engineers, Division St, Paper 1188, LXXXIII, (March, 1957), 83.

10. Davisson, M. T. "Behavior of Flexible Vertical Piles Subjected to Moment, Shear, and Axial Loads." Ph.D. Thesis, University of Illinois, 1960.

11. Griffith, J. R. "Construction Design Charts." Western Construction News, Vol. 14, No. 10, p. 350, 1939.

12. Hurst, H. T. and J. P. H. Mason, Jr. "Resistance of Steel- and Wood-Pole Foundations to Uplifting and Overturning Forces." Virginia Agricultural Experiment Station Report No. 28, 1959.

13. Kondner, R. L. and Raymond J. Krizek. "Correlation of Load Bearing Tests on Soils." Highway Research Board Proceedings, Vol. 41, pp. 557-590, 1962.

14. Kondner, Robert L. and Gordon E. Green. "Lateral Stability of Rigid Poles Subjected to a Ground-Line Thrust." Highway Research Board, Bulletin 342, 1962.

15. Kondner, Robert L. and J. A. Cunningham. "Lateral Stability of Rigid Poles Partially Embedded in Sand." Highway Research Board Abstracts. Vol. 32, December, 1962.

16. Kondner, Robert L., R. J. Krizek, and B. B. Schimming. "Lateral Stability of Rigid Poles Subjected to an Applied Couple." Technical Report, Civil Engineering Department, Northwestern University, 1962.

17. Krynine, D. P. "Landslides and Pile Action." Engineering News Record, Vol. 107, p. 860, 1931.

18. Langhaar, H. L. Dimensional Analysis and Theory of Models. New York: John Wiley and Sons, Inc., 1957.

19. Means, R. E. and J. V. Parcher. Physical Properties of Soils. Columbus, Ohio: Charles E. Merrill Books, Inc., 1963.

20. Murphy, G. Similitude in Engineering. New York: The Ronald Press, 1950.

21. Nakamura, M. "Uber Den Erdwiderstand Gegen Maste Unter Besonderer Berucksichtigung Der Zusammendruckbarkeit Des Bondens." Bauingenieur, Vol. 16, No. 21/24, pp. 269-275, 1935.

22. Nelidov, I. M. "Finding Depth of Footing for a Pole Subjected to Lateral Loads." Civil Engineering, Vol. 28, p. 196. Discussion p. 527, 767, 1958.

23. Nelson, G. L., G. W. A. Mahoney, and J. I. Fryrear. "Stability of Poles Under Tilting Moments," Part I. Agricultural Engineering 39:(3) 166-170, March, 1958.

24. Nelson, G. L. "Stability of Poles Under Tilting Moments." Part II. Agricultural Engineering 39:(4) 226-230, April, 1958.

25. Osterberg, J. O. "Lateral Stability of Poles Embedded in a Clay Soil." Unpublished Report, The Technological Institute, Northwestern University.

26. Patterson, Donald. How to Design Pole-Type Buildings. American Wood Preserver's Institute. 1957.

27. Prakash, S. "A Review of the Behavior of Partially Embedded Poles Subjected to Lateral Loads." M.S. Thesis, University of Illinois, 1960.

28. Rice, Charles. "A Model Study of Anchorage Types for Fixed-End Arches." Unpublished Report, Agricultural Engineering Department, Oklahoma State University, Stillwater, Oklahoma, 1959.

29. Robbins, N. G. "Piers Supported by Passive Pressures." Civil Engineering, Vol. 27, p. 276, 1957.

30. Rutledge, P. C. Chart for Embedment of Posts With Overturning Loads. Chicago: Outdoor Advertising Association of America, Inc., 1947.

31. Seiler, J. F. "Effect of Depth of Embedment on Pole Stability." Wood Preserving News, Vol. X, No. 11, p. 152-161. November, 1932.

32. Shilts, Walter S., Leroy D. Graves, and George G. Driscoll. "A Report of Field and Laboratory Tests on the Stability of Posts Against Lateral Loads." Proceedings of the Second International Conference on Soil Mechanics, Rotterdam, 1948.

33. Terzaghi, K., "Evaluation of Coefficients of Subgrade Reaction." Geotechnique, Vol. 4, December, 1955.

34. Terzaghi, K. and R. B. Peck, Soil Mechanics in Engineering Practice. New York: John Wiley and Sons, Inc., 1948.

35. Walker, J. N. and E. H. Cox. "Design of Pier Foundations for Lateral Loads." American Society of Agricultural Engineers, Paper No. 64-408, Ft. Collins, Colorado, 1964.

36. Williams, T. E. H. "Soil Failure During Overturning of Piles." Engineering (London) Vol. 173, p. 134, 1952.

APPENDIX A

EXPERIMENTAL DATA FOR MODEL PIERS

APPENDIX A-1

DATA FOR MODEL TEST WHEN π_2 WAS 4
AND π_3 WAS 1.446

Elapsed Time Minutes	π_4 $KG\rho t/H$	π_1 = Tan Θ (Average)				
		$\pi_5 = 1$	$\pi_5 = 2$	$\pi_5 = 3$	$\pi_5 = 4$	$\pi_5 = 5$
.5	.0348	.0054	.0077	.0091	.0107	.0126
1	.0697	.0058	.0078	.0092	.0107	.0126
2	.1395	.0064	.0079	.0093	.0108	.0128
3	.2093	.0066	.0080	.0094	.0109	.0129
4	.2790	.0069	.0082	.0096	.0109	.0129
5	.3488	.0071	.0081	.0096	.0110	.0129
6	.4186	.0072	.0084	.0097	.0111	.0130
8	.5581	.0076	.0086	.0098	.0111	.0131
8.57	.5980	.0077	.0087	.0098	.0111	.0131
Rebound		.0056	.0075	.0093	.0096	.0117

APPENDIX A-2

DATA FOR MODEL TEST WHEN π_2 WAS 5
AND π_3 WAS 1.446

Elapsed Time Minutes	π_4 KGρt/H	π_1 = Tan Θ (Average)				
		π_5 = 1	π_5 = 2	π_5 = 3	π_5 = 4	π_5 = 5
.5	.0279	.0092	.0183	.0203	.0217	.0227
1	.0558	.0101	.0187	.0204	.0218	.0228
2	.1116	.0140	.0189	.0207	.0219	.0229
3	.1674	.0146	.0190	.0208	.0220	.0229
4	.2232	.0162	.0194	.0209	.0221	.0230
5	.2791	.0160	.0195	.0209	.0222	.0230
6	.3349	.0167	.0197	.0210	.0222	.0230
8	.4465	.0170	.0198	.0211	.0224	.0230
10	.5582	.0174	.0199	.0213	.0225	.0230
10.71	.5980	.0175	.0200	.0213	.0225	.0231
Rebound		.0140	.0173	.0177	.0198	.0210

APPENDIX A-3

DATA FOR MODEL TEST WHEN π_2 WAS 6
AND π_3 WAS 1.446

Elapsed Time Minutes	π_4 KGρt/H	π_1 = Tan θ (Average)				
		$\pi_5 = 1$	$\pi_5 = 2$	$\pi_5 = 3$	$\pi_5 = 4$	$\pi_5 = 5$
.5	.0232	.0279	.0435	.0485	.0518	.0543
1	.0465	.0328	.0442	.0489	.0519	.0545
2	.0930	.0330	.0448	.0491	.0523	.0548
3	.1416	.0344	.0453	.0493	.0525	.0548
4	.1882	.0356	.0455	.0495	.0526	.0550
5	.2347	.0368	.0458	.0497	.0528	.0550
6	.2812	.0374	.0461	.0498	.0529	.0551
8	.3742	.0387	.0463	.0500	.0530	.0551
10	.4651	.0395	.0465	.0502	.0532	.0553
12	.5602	.0401	.0467	.0503	.0533	.0553
12.85	.5980	.0403	.0468	.0504	.0533	.0553
Rebound		.0354	.0461	.0461	.0491	.0521

APPENDIX A-4

DATA FOR MODEL TEST WHEN π_2 WAS 7
AND π_3 WAS 1.446

Elapsed Time Minutes	π_4 KGρt/H	π_1 = Tan Θ (Average)				
		$\pi_5 = 1$	$\pi_5 = 2$	$\pi_5 = 3$	$\pi_5 = 4$	$\pi_5 = 5$
.25	.0099	.0355	.0488	.0536	.0580	.0583
.50	.0199	.0381	.0495	.0545	.0583	.0585
.75	.0298	.0392	.0498	.0546	.0584	.0587
1	.0398	.0403	.0502	.0547	.0585	.0587
2	.0797	.0417	.0508	.0551	.0588	.0590
3	.1196	.0433	.0513	.0553	.0589	.0592
4	.1594	.0438	.0514	.0554	.0591	.0592
5	.1993	.0442	.0517	.0554	.0592	.0593
6	.2392	.0448	.0520	.0555	.0592	.0594
8	.3189	.0451	.0524	.0557	.0594	.0595
10	.3987	.0455	.0525	.0558	.0594	.0596
12	.4784	.0459	.0526	.0558	.0596	.0596
14	.5581	.0462	.0528	.0558	.0595	.0596
15	.5980	.0470	.0535	.0559	.0595	.0596
Rebound		.0404	.0479	.0537	.0542	.0571

APPENDIX A-4

(Continued)

Elapsed Time Minutes	π_4 KGρt/H	π_1 = Tan Θ (Average)			
		$\pi_5 = 6$	$\pi_5 = 7$	$\pi_5 = 8$	$\pi_5 = 9$
.25	.0099	.0604	.0624	.0633	.0661
.50	.1999	.0606	.0627	.0635	.0662
.75	.0298	.0608	.0628	.0635	.0663
1	.0398	.0608	.0629	.0635	.0663
2	.0797	.0611	.0630	.0637	.0664
3	.1196	.0611	.0631	.0639	.0664
4	.1594	.0612	.0632	.0639	.0665
5	.1993	.0612	.0632	.0640	.0665
6	.2392	.0613	.0633	.0641	.0665
8	.3189	.0614	.0634	.0641	.0665
10	.3987	.0615	.0635	.0641	.0666
12	.4784	.0615	.0635	.0641	.0666
14	.5581	.0615	.0636	.0641	.0666
15	.5980	.0615	.0636	.0641	.0666
Rebound		.0575	.0603	.0619	.0640

APPENDIX A-5

DATA FOR MODEL TEST WHEN π_2 WAS 8
AND π_3 WAS 1.446

Elapsed Time Minutes	π_4 KGρt/H	π_1 = Tan Θ (Average)				
		π_5 = 1	π_5 = 2	π_5 = 3	π_5 = 4	π_5 = 5
.5	.0174	.0423	.0607	.0667	.0691	.0709
1	.0348	.0455	.0610	.0670	.0694	.0710
2	.0697	.0505	.0623	.0675	.0694	.0713
3	.1046	.0529	.0628	.0675	.0696	.0713
4	.1395	.0518	.0631	.0677	.0698	.0713
5	.1744	.0520	.0634	.0678	.0698	.0714
6	.2093	.0531	.0635	.0679	.0699	.0715
8	.2790	.0540	.0640	.0681	.0700	.0716
10	.3488	.0545	.0643	.0683	.0701	.0716
12	.4186	.0555	.0646	.0683	.0701	.0717
14	.4883	.0560	.0648	.0684	.0702	.0717
16	.5580	.0564	.0650	.0685	.0703	.0717
17.14	.5980	.0565	.0652	.0686	.0703	.0717
Rebound		.0500	.0593	.0650	.0661	.0679

APPENDIX A-6

DATA FOR MODEL TEST WHEN π_2 WAS 9
AND π_3 WAS 1.446

Elapsed Time Minutes	π_4 KGρt/H	π_1 = Tan θ (Average)				
		$\pi_5 = 1$	$\pi_5 = 2$	$\pi_5 = 3$	$\pi_5 = 4$	$\pi_5 = 5$
.5	.0155	.0447	.0661	.0765	.0823	.0859
1	.0310	.0498	.0680	.0770	.0829	.0862
2	.0620	.0630	.0682	.0775	.0834	.0864
3	.0930	.0546	.0694	.0779	.0839	.0866
4	.1240	.0559	.0698	.0782	.0841	.0867
5	.1550	.0561	.0708	.0783	.0843	.0868
6	.1860	.0573	.0705	.0785	.0845	.0869
8	.2460	.0578	.0710	.0788	.0848	.0871
10	.3101	.0590	.0714	.0790	.0850	.0871
12	.3720	.0595	.0716	.0792	.0852	.0872
14	.4341	.0601	.0718	.0793	.0853	.0873
16	.4961	.0605	.0721	.0794	.0854	.0873
18	.5581	.0610	.0724	.0795	.0855	.0874
19.28	.5980	.0611	.0724	.0795	.0856	.0874
Rebound		.0521	.0570	.0724	.0802	.0832

APPENDIX A-7

DATA FOR MODEL TEST WHEN π_2 WAS 7 AND π_3 WAS .4820

Elapsed Time Minutes	π_4 KGρt/H	π_1 = Tan Θ (Average)				
		π_5 = 1	π_5 = 2	π_5 = 3	π_5 = 4	π_5 = 5
.5	.0199	.0021	.0024	.0025	.0026	.0023
1	.0398	.0022	.0024	.0025	.0026	.0027
2	.0797	.0023	.0024	.0025	.0026	.0027
3	.1196	.0023	.0024	.0025	.0026	.0027
4	.1594	.0024	.0025	.0026	.0026	.0027
5	.1993	.0024	.0026	.0026	.0026	.0027
6	.2392	.0024	.0025	.0026	.0026	.0027
8	.3189	.0024	.0025	.0026	.0027	.0027
10	.3987	.0026	.0025	.0026	.0027	.0027
12	.4784	.0026	.0026	.0026	.0027	.0027
14	.5581	.0026	.0026	.0026	.0027	.0027
15	.5980	.0027	.0026	.0026	.0027	.0027
Rebound		.0015	.0017	.0019	.0017	.0018

APPENDIX A-8

DATA FOR MODEL TEST WHEN π_2 WAS 7
AND π_3 WAS .9640

Elapsed Time Minutes	π_4 KGρt/H	π_1 = Tan Θ (Average)				
		π_5 = 1	π_5 = 2	π_5 = 3	π_5 = 4	π_5 = 5
.5	.0199	.0099	.0150	.0169	.0183	.0188
1	.0398	.0111	.0151	.0170	.0185	.0190
2	.0797	.0120	.0154	.0174	.0185	.0190
3	.1196	.0126	.0156	.0175	.0186	.0190
4	.1594	.0130	.0157	.0176	.0186	.0190
5	.1993	.0132	.0157	.0177	.0187	.0190
6	.2392	.0134	.0158	.0177	.0187	.0190
8	.3189	.0136	.0159	.0177	.0187	.0190
10	.3987	.0136	.0159	.0178	.0188	.0191
12	.4784	.0138	.0160	.0179	.0188	.0191
14	.5581	.0138	.0161	.0178	.0188	.0192
15	.5980	.0138	.0161	.0179	.0188	.0192
Rebound		.0109	.0134	.0159	.0154	.0168

APPENDIX A-9

DATA FOR MODEL TEST WHEN π_2 WAS 7
and π_3 WAS 1.9280

Elapsed Time Minutes	π_4 KGρt/H	π_1 = Tan θ (Average)				
		$\pi_5 = 1$	$\pi_5 = 2$	$\pi_5 = 3$	$\pi_5 = 4$	$\pi_5 = 5$
.5	.0199	.0362	.0784	.0954	.1055	.1147
1	.0398	.0535	.0804	.0962	.1061	.1153
2	.0797	.0552	.0830	.0972	.1070	.1154
3	.1196	.0576	.0842	.0980	.1076	.1159
4	.1594	.0594	.0856	.0985	.1079	.1161
5	.1993	.0606	.0864	.0992	.1083	.1162
6	.2392	.0619	.0869	.0995	.1085	.1163
8	.3189	.0637	.0878	.1002	.1087	.1167
10	.3987	.0653	.0888	.1008	.1092	.1169
12	.4784	.0661	.0895	.1012	.1095	.1171
14	.5581	.0679	.0900	.1017	.1099	.1172
15	.5980	.0684	.0903	.1018	.1099	.1173
Rebound		.0612	.0817	.0947	.1030	.1119

APPENDIX A-10

DATA FOR MODEL TEST WHEN π_2 WAS 7
AND π_3 WAS 2.410

Elapsed Time Minutes	π_4 KGρt/H	π_1 = Tan θ (Average)				
		$\pi_5 = 1$	$\pi_5 = 2$	$\pi_5 = 3$	$\pi_5 = 4$	$\pi_5 = 5$
.5	.0199	.0791	.0924	.1043	.1125	.1183
1	.0398	.0732	.0936	.1055	.1133	.1189
2	.0797	.0768	.0950	.1067	.1144	.1196
3	.1196	.0788	.0962	.1073	.1148	.1198
4	.1594	.0803	.0965	.1080	.1148	.1200
5	.1993	.0816	.0972	.1078	.1149	.1202
6	.2392	.0826	.0974	.1084	.1153	.1205
8	.3189	.0841	.0981	.1090	.1156	.1206
10	.3987	.0853	.0987	.1093	.1158	.1207
12	.4784	.0863	.0992	.1097	.1160	.1210
14	.5581	.0872	.0995	.1099	.1161	.1210
15	.5980	.0876	.0998	.1100	.1162	.1210
Rebound		.0721	.0920	.1023	.1082	.1143

APPENDIX B

EXPERIMENTAL DATA FOR PROTOTYPE

APPENDIX B-1

DATA FOR PROTOTYPE TEST WHEN π_2 WAS 7 AND π_3 WAS 0.9943

Elapsed Time Minutes	π_4 KGρt/H	π_1 = Tan Θ (Average)				
		π_5 = 1	π_5 = 2	π_5 = 3	π_5 = 4	π_5 = 5
.5	.0099	.0113	.0165	.0191	.0204	.0217
1	.0199	.0133	.0169	.0192	.0205	.0219
2	.0398	.0118	.0173	.0195	.0208	.0220
3	.0597	.0122	.0176	.0196	.0209	.0221
4	.0796	.0123	.0176	.0198	.0210	.0221
5	.0995	.0126	.0177	.0198	.0210	.0221
6	.1194	.0127	.0177	.0198	.0210	.0222
8	.1592	.0127	.0179	.0198	.0210	.0222
10	.1990	.0128	.0180	.0199	.0210	.0222
12	.2388	.0130	.0180	.0199	.0210	.0223
15	.2985	.0131	.0181	.0200	.0212	.0224
Rebound		.0090	.0136	.0161	.0178	.0190

APPENDIX B-2

DATA FOR PROTOTYPE TEST WHEN π_2 WAS 7
AND π_3 WAS 1.2429

Elapsed Time Minutes	π_4 KGρt/H	π_1 = Tan θ (Average)				
		$\pi_5 = 1$	$\pi_5 = 2$	$\pi_5 = 3$	$\pi_5 = 4$	$\pi_5 = 5$
.5	.0099	.0067	.0235	.0313	.0366	.0407
1	.0199	.0072	.0244	.0320	.0372	.0411
2	.0398	.0107	.0252	.0326	.0375	.0414
3	.0597	.0136	.0258	.0328	.0378	.0417
4	.0796	.0148	.0262	.0333	.0381	.0418
5	.0995	.0156	.0264	.0335	.0382	.0419
6	.1194	.0163	.0267	.0337	.0383	.0421
8	.1592	.0174	.0272	.0341	.0385	.0421
10	.1990	.0182	.0277	.0345	.0388	.0422
12	.2388	.0192	.0280	.0346	.0390	.0424
15	.2985	.0202	.0285	.0348	.0392	.0425
Rebound		.0145	.0221	.0292	.0337	.0371

APPENDIX B-3

DATA FOR PROTOTYPE TEST WHEN π_2 WAS 7 AND π_3 WAS 2.9835

Elapsed Time Minutes	π_4 KGρt/H	π_1 = Tan Θ (Average)				
		$\pi_5 = 1$	$\pi_5 = 2$	$\pi_5 = 3$	$\pi_5 = 4$	$\pi_5 = 5$
.5	.0099	.0134	.0276	.0330	.0366	.0404
1	.0199	.0156	.0282	.0334	.0372	.0408
2	.0398	.0172	.0288	.0338	.0376	.0412
3	.0597	.0188	.0294	.0344	.0376	.0410
4	.0796	.0200	.0296	.0346	.0380	.0416
5	.0995	.0206	.0300	.0348	.0382	.0418
6	.1194	.0214	.0304	.0350	.0384	.0418
8	.1592	.0226	.0306	.0352	.0388	.0420
10	.1990	.0238	.0308	.0354	.0395	.0422
12	.2388	.0246	.0312	.0358	.0395	.0422
15	.2985	.0255	.0314	.0360	.0395	.0422
Rebound		.0150	.0192	.0246	.0286	.0321

APPENDIX B-4

DATA FOR PROTOTYPE TEST WHEN π_2 WAS 7 AND π_3 WAS 3.978

Elapsed Time Minutes	π_4 KGρt/H	π_1 = Tan Θ (Average)				
		π_5 = 1	π_5 = 2	π_5 = 3	π_5 = 4	π_5 = 5
.5	.0099	.0450	.0774	.0960	.1192	.1374
1	.0199	.0500	.0800	.0972	.1212	.1388
2	.0398	.0544	.0816	.0984	.1244	.1410
3	.0597	.0568	.0828	.0994	.1250	.1414
4	.0796	.0586	.0839	.1002	.1264	.1418
5	.0995	.0602	.0844	.1004	.1270	.1420
6	.1194	.0612	.0852	.1010	.1280	.1422
8	.1592	.0630	.0882	.1016	.1286	.1444
10	.1990	.0644	.0872	.1020	.1294	.1448
12	.2388	.0658	.0876	.1022	.1300	.1450
15	.2985	.0672	.0884	.1026	.1320	.1460
Rebound		.0566	.0762	.0928	.1172	.1304

VITA

George Burns Welch

Candidate for the Degree of

Doctor of Philosophy

Thesis: EXPERIMENTAL ANALYSIS OF ROTATION IN A VERTICAL PLANE OF SHALLOW PIER FOUNDATIONS SUBJECTED TO A COUPLE

Major Field: Agricultural Engineering

Biographical:

Personal Data: Born near Soso, Mississippi, November 23, 1920, the son of James W. and Arrilla Welch.

Education: Graduated from Soso High School, located in Soso, Mississippi, in May, 1939; attended Jones County Junior College, Ellisville, Mississippi, and Mississippi State University as an undergraduate; received the Bachelor of Science degree from Mississippi State University in 1947, with a major in Agricultural Engineering; received the Master of Science degree from Texas Agricultural and Mechanical College in 1950 with a major in Agricultural Engineering; completed the requirements for the Doctor of Philosophy degree from Oklahoma State University in August, 1965.

Professional Experience: Entered the Army Air Force in September, 1942, and served three years on active duty, taught in the Agriculture Department at Jones County Junior College from August, 1947, to June, 1948; taught and conducted research work in the Agricultural Engineering Department at Mississippi State University from June, 1948, to September, 1949, and from January, 1951, to September, 1962; served as a graduate research assistant for the Agricultural Engineering Department, Oklahoma State University from September, 1962, to May, 1965.

Professional Organizations: American Society of Agricultural Engineers.